SOLUTION OF THE TWO-POINT BOUNDARY VALUE PROBLEMS OF OPTIMAL SPACECRAFT ROTATIONAL MANEUVERS

by

Srinivas Rao Vadali

Dissertation submitted to the Faculty of the

Virginia Polytechnic Institute and State University

in partial fulfillment of the requirements for

the degree of

DOCTOR OF PHILOSOPHY

in

Engineering Mechanics

APPROVED:

J. L. Junkins

J. A. Burns

L. G. Kraige

L. Meirovitch

D. T. Mook

December, 1982
Blacksburg, Virginia

ACKNOWLEDGEMENTS

I wish to acknowledge the friendship and guidance of Dr. John L. Junkins during the course of this research. The education that I derived from his knowledge of dynamics, controls, and human relations would keep me in good stead for years to come.

Special thanks are due to Dr. L. Glenn Kraige for many valuable suggestions and helpful discussions on a variety of subjects.

The excellent typing skills and patience of Ms. Vanessa McCoy are gratefully appreciated.

TABLE OF CONTENTS

LIST OF FIGURES

CHAPTER 1

INTRODUCTION

Satellites launched by conventional launch vehicles are often initially spin stabilized in orbit. The advent of the space shuttle has decreased the need for spin-stabilization, but imperfect launch conditions could induce arbitrary tumbling motions. In any case, a final attitude acquisition maneuver is necessary to despin (detumble) and reorient the spacecraft to a three-axis controlled mode, the general mode of operation for communications satellites. The next generation of space systems will be required to maintain spacecraft orientation precise to a few arc-seconds due to the increasingly stringent requirements on pointing accuracy, the success of which depends on the performance of various sensors, actuators, and control laws implemented onboard. The angles interlocking star sensors to terrain sensors, for example, need on-orbit calibration from time to time; for this and other reasons, the continuing need for occasional large angle rotational maneuvers is evident.

Attitude control systems currently in use can be broadly classified under two categories: those using external torques generated by mass expulsion, environmental electomagnetic field interactions or solar radiation pressure etc., and momentum exchange devices like reaction wheels and control moment gyros which generate internal torques. Attitude stabilization, which can be thought of as small angle attitude control, has been studied with the available control systems either singly or in combination, by numerous authors [1-4]. A number of feasible large angle maneuver strategies for rigid spacecraft have been

proposed by Gebman and Mingori [5], Barba and Aubrun [6], Junkins [7], Cochran and Junkins [8], and Meyer [9]. Junkins and Turner [10] have treated optimal large angle maneuvers based on an integral performance index of the sum squares of the external torques. Skaar and Kraige [11,12], and Skaar [13] recently considered optimal large angle maneuvers of reaction wheel systems, which minimize an integral of the sum squares of the individual wheel powers, and include admissible control torque inequality constraints.

Application of optimal control theory to the dynamic model of a system leads to a system of differential equations, whose order is twice that of the original system. Moreover, the boundary conditions on the states of the augmented system are typically split (in the sense that some are specified at the initial time and some at the final time), thereby precluding direct numerical integration. The augmented system with such split boundary conditions constitutes a two-point boundary value problem (TPBVP). Only under special conditions do these TPBVPs admit analytical closed form solutions. Numerical solution of the TPBVPs is not straightforward and requires judicious selection of a method and considerable insight into the problem at hand. A number of techniques for solving TPBVPs has been proposed in recent years [14,15]. This is not surprising, due not only to the intensity of effort put forth by different researchers, but also due to the fact that no single numerical method works efficiently for all TPBVPs. It is rather unfortunate that one still finds relatively few applications to the optimal control computations for large nonlinear systems.

This dissertation has been motivated by the desire to study many hitherto unsolved problems of optimal large angle attitude maneuvers of rigid spacecraft. It is organized into five subsequent chapters. Chapter II treats the numerical solution of TPBVPs. Several commonly used algorithms are presented and applications are illustrated via numerical examples. Chapter III is based on the formulation of the rigid body optimal maneuver problem of Junkins and Turner [10]. New insights into the problem are arrived at, which greatly simplify the numerical solutions. In addition an example maneuver is solved by two different numerical schemes.

In Chapter IV, the optimal control problem of asymmetric spacecraft and reaction wheel systems are formulated. Numerical examples are presented for two different spacecraft configurations. This chapter forms the central piece which ties the subsequent developments in this dissertation with the material in [10]. Chapter V presents a mathematical extension of the formulations presented in Chapters III and IV, for maneuvers with both internal and external torques. A numerical example is presented for an optimal maneuver with an integral performance index involving the control torques. Chapter VI summarizes the developments and results of the previous chapters and recommends areas of further study.

CHAPTER II

NUMERICAL SOLUTION OF TWO POINT BOUNDARY VALUE PROBLEMS

In this chapter, some of the available numerical methods for the solution of two-point boundary value problems (TPBVPs) in nonlinear ordinary differential equations are presented. Applications of these methods are illustrated via numerical examples. TPBVPs arising from the application of either classical variational calculus or the Pontryagin's principle (Appendix A) to mathematical models of dynamic systems are sometimes stiff (in the sense that some particular solutions of the differential equations grow while others decay rapidly). Solutions obtained by numerical integration of stiff differential equations suffer from often unacceptably large errors unless sophisticated algorithms designed specifically for these problems are used. A simple stiff system (however, it does not stem from an optimal control problem) is considered in Example 2.1. The second example considered is an optimal detumble (nonlinear) maneuver of a rigid asymmetric spacecraft and is non-stiff.

A number of methods for the numerical solution of TPBVPs are currently available. They can be classified under the following categories:

- Quasi-linearization
- Shooting methods
- Polynomial approximation methods
- Finite difference methods

Of these methods, quasi-linearization, shooting methods, polynomial

approximation, and combination methods are discussed here. An excellent treatment of finite difference methods can be found in [16]. The discussion in this chapter is centered around a class of TPBVPs which arise in spacecraft optimal control applications. In subsequent chapters, we use these methods (and related methods) to solve for more difficult maneuvers typical of those encountered in practice. More general formulations are presented by Miele [17] and more recently by Blank and Shinar [18]. These formulations include equality and inequality constraints (both differential and non-differential) on the states, controls, and model parameters of the system.

2.1 FORMULATION OF THE PROBLEM

Let the TPBVP be given by the following sets of state ($\underline{x}$) and co-state ($\underline{\lambda}$) vector nonlinear differential equations:

$$\dot{\underline{x}} = \underline{g}(\underline{x}, \underline{\lambda}, t), \text{ (n equations)}$$

$$\dot{\underline{\lambda}} = \underline{h}(\underline{x}, \underline{\lambda}, t), \text{ (n equations)} \tag{2.1}$$

For a well-posed problem, we need 2n boundary conditions for the solution to Eq. (2.1). The boundary conditions are

$$\underline{x}(0) = \underline{\alpha} \text{ (n initial conditions)} \tag{2.2}$$

and

$$\underline{\psi}\,(\underline{x}(T), \underline{\lambda}(T)) = 0 \text{ (n final conditions)}, \tag{2.3}$$

where $\underline{\alpha}$ is a known constant vector and ψ_i can either be a linear or nonlinear function. Analytical solutions of these equations do not exist except for special cases. On the other hand, the split boundary conditions are incomplete such that numerical integration (forward or backward) is not possible. For the purpose of generalization, we define

the augmented 2n vector $\underline{X}$, such that

$$\underline{X} = [x_1\ x_2 \cdots x_n\ \lambda_1\ \lambda_2 \cdots \lambda_n]^T \tag{2.4}$$

and re-write the TPBVP as

$$\dot{\underline{X}} = \underline{f}(\underline{X},t) \tag{2.5}$$

with boundary conditions

$$X_i(0) = \alpha_i \quad , \quad i = 1,2, \ldots n \tag{2.6}$$

and

$$\underline{\psi}\ (\underline{X}(T)) = 0 \tag{2.7}$$

Brief descriptions of various numerical methods for the solution of the TPBVP are presented next.

2.2 QUASI-LINEARIZATION

Quasi-linearization is a generalization of the function space Newton-Raphson method in Banach space [14].

Equations (2.5) are linearized about a nominal solution ($\underline{X}^k(t)$) for the k^{th} trial solution (i.e., the right-hand sides of Eqs. (2.5) are expanded in a Taylor's series and only first-order terms are retained). The linearized equations are given by

$$\dot{\underline{X}}^k(t) + \Delta\dot{\underline{X}}^k(t) = \underline{f}(\underline{X}^k,t) + \left.\frac{\partial \underline{f}(\underline{X},t)}{\partial \underline{X}}\right|_{\underline{X}^k(t)} \Delta\underline{X}^k \tag{2.8}$$

where $\Delta X_i^k(t)$ are corrections (departure motion) to the nominal trial trajectories. If $\underline{X}^k(t)$ is selected such that the initial conditions of Eq. (2.6) are satisfied exactly but the final conditions of Eq. (2.7) are satisfied only approximately, the following boundary conditions are then applicable on $\Delta\underline{X}^k(t)$:

$$\Delta X_i^k(0) = 0 \quad , \quad i = 1,2, \ldots, n, \tag{2.9}$$

$$\frac{\partial \underline{\psi}}{\partial \underline{X}}\Big|_{\underline{X}^k(T)} \Delta \underline{X}^k(T) + \underline{\psi}(\underline{X}^k(T)) = 0 \tag{2.10}$$

Since $\underline{X}^k(t)$ is a known (typically, tabular) function, $\dot{\underline{X}}^k(t)$ can be approximated direc ly by numerical differentiation; it is also a simple matter of substitution to recalculate $\underline{f}(\underline{X}^k, t)$. Notice that if $\underline{X}^k(t)$ is obtained by direct integration of Eq. (2.1) with the given initial conditions of Eq. (2.2) and current estimates for the unspecified initial conditions, Eq. (2.8) can be written as

$$\Delta \dot{\underline{X}}^k(t) = [F^k(t)]\Delta \underline{X}^k(t) \tag{2.11}$$

$$[F^k(t)] = \left[\frac{\partial \underline{f}}{\partial \underline{\dot{X}}}\Big|_{\underline{X}^k(t)}\right] \tag{2.12}$$

and the boundary conditions of Eqs. (2.9) and (2.10) still hold. This variation avoids numerical differentiation; the differential equations are homogeneous, but at each iteration, the non-linear equations (2.5) have to be integrated to obtain $\underline{X}^k(t)$. The nominal solution for the next iteration is given by

$$\underline{X}^{k+1}(t) = \underline{X}^k(t) + \Delta \underline{X}^k(t) \tag{2.13}$$

However, to use Eq. (2.11) again, in lieu of Eq. (2.8), we should apply Eq. (2.13) only at the initial time and numerically integrate Eq. (2.5) to obtain a new nominal. A second variation of the method is to substitute Eq. (2.13) in Eq. (2.8) so that

$$\dot{\underline{X}}^{k+1}(t) = [F^k(t)]\underline{X}^{k+1} + \{f(\underline{X}^k(t), t) - [F^k(t)]\underline{X}^k(t)\} \tag{2.14}$$

This variation also avoids numerical differentiation, but the nonlinear equations do not have to be integrated at each iteration. The

linearized differential equations are non-homogeneous; the boundary conditions on $\underline{X}^{k+1}(t)$ are given by

$$x_i^{k+1}(0) = \alpha_i \quad , \quad i = 1,2,\ldots n, \tag{2.15}$$

$$\left[\frac{\partial \psi}{\partial \underline{X}}\Big|_{\underline{X}^k(T)}\right] \underline{X}^{k+1}(T) = - \left\{\left[\frac{\partial \psi}{\partial \underline{X}}\Big|_{\underline{X}^k(T)}\right] \underline{X}^k(T) + \underline{\psi}(\underline{X}^k(T))\right\} \tag{2.16}$$

Regardless of the variation used, we in essence solve a linear TPBVP at each iteration. Theoretically, these solutions converge in the limit to the solution of the nonlinear TPBVP. Roberts and Shipman [14] present sufficient conditions for convergence of quasi-linearization, and estimates of the rate of convergence and accuracy of the solution using Kantorovitch's theorem. For practical purposes, we accept the solutions as converged to a specific tolerance ε if the relative error satisfies

$$\frac{\|\underline{X}^{k+1}(t) - \underline{X}^k(t)\|}{\|\underline{X}^k(t)\|} < \varepsilon \quad , \quad 0 \leq t \leq T \tag{2.17}$$

for each integration step. The linear TPBVP at each iteration is solved either by shooting methods or polynomial approximation methods.

2.3 SHOOTING METHODS

Shooting methods are iterative methods for adjusting missing initial conditions so that the errors in the terminal boundary conditions in Eq. (2.2) are driven to zero. In this category are method of adjoints and method of complementary functions [14], methods of particular solutions [19], and a method using state transition matrix algorithms and differential corrections [20]. The methods of adjoints

and differential corrections are directly applicable to nonlinear problems whereas the other two methods are based on superposition and are thus valid for locally linear problems (nonlinear problems are solved by combining these ideas with quasi-linearization [21]).

2.3.1 METHOD OF PARTICULAR SOLUTIONS

The method of particular solutions is summarized here. Consider the linear system of equations:

$$\underline{\dot{X}} = [F(t)]\underline{X} + \underline{D}(t) \tag{2.18}$$

with the boundary conditions

$$X_i(0) = \alpha_i \quad , \quad i = 1,2,\ldots,n, \tag{2.19}$$

$$[V]\underline{X}(T) = \underline{\beta} \tag{2.20}$$

where [V] is a known [n x 2n] matrix and $\underline{\beta}$ is a known constant vector. Let

$$\underline{X}^j = \underline{X}^j(t) \quad j = 1,2,\ldots,n+1 \tag{2.21}$$

denote n+1 particular solutions obtained by forward numerical solution of Eq. (2.18) with the following n+1 sets of initial conditions:

$$X_i^j(0) = \alpha_i \quad , \quad i = 1,2,\ldots,n, \quad j = 1,2,\ldots,n+1$$

$$X_{n+k}^j(0) = \delta_{jk} \quad , \quad k = 1,2,\ldots,n \quad , \quad j = 1,2,\ldots,n+1 \tag{2.22}$$

where δ_{jk} is the Kronecker delta. Since the differential equation (2.18) is linear, we can superimpose the n+1 particular solutions to obtain another solution

$$\underline{X}(t) = \sum_{j=1}^{n+1} k_j \underline{X}^j(t) \tag{2.23}$$

The unknown coefficients (k_j) are determined in such a fashion that the solution of Eq. (2.23) satisfies the boundary conditions of Eqs. (2.22). Substituting Eq. (2.23) in the initial conditions of Eq. (2.15), we obtain the side condition:

$$\sum_{j=1}^{n+1} k_j = 1 \tag{2.24}$$

Similarly, the terminal conditions of Eq. (2.20) yield the n equations

$$[V] \sum_{j=1}^{n+1} k_j \underline{X}^j(T) = \underline{\beta} \tag{2.25}$$

Equations (2.24) and (2.25) constitute n+1 equations which can be solved to determine the n+1 k_j's. The solution to the linearized TPBVP is then obtained by recombining the individual particular solutions according to Eq. (2.23). This is algorithm A. Notice that if Eq. (2.11) is used for the linearized TPBVP, due to the nature of the initial conditions in Eq. (2.9), the $n+1^{th}$ departure motion is zero. Thus, the $n+1^{th}$ particular solution obtained from Eq. (2.13) remains unchanged since Eq. (2.11) is homogeneous. Furthermore, the particular solutions need not be stored; only the state at the initial and final times need be retained. Each iteration involves nonlinear integration of the updated nominal trajectory which will agree exactly with Eq. (2.23) only for the case that the implicit linearization causes negligible errors. This is algorithm B.

2.3.2 METHOD OF DIFFERENTIAL CORRECTIONS

This method iteratively refines the initial co-state estimates based on the error in the terminal conditions. It is convenient to use the formulation given by Eqs. (2.1-2.3) most of the time. The algorithm is summarized in the following steps.

a. The n unspecified initial co-states are selected and Eqs. (2.1) is integrated forward in time ($0 \leq t \leq T$), perhaps (depending upon the particular variation of this method) storing the nominal trajectory $x_i(t)$ and $\hat{\lambda}_i(t)$ along the way. At the final time, $\|\underline{\psi}(\hat{\underline{x}}(T), \hat{\underline{\lambda}}(T))\|$ is computed; if it is zero, it is not necessary to proceed further.

b. Before proceeding to step c, the state transition matrix $\Phi(t,0)$ for the system of Eqs. (2.1) has to be computed along the nominal trajectories. $\Phi(t,0)$ which maps admissible initial condition variations into the first order predicted variations at time t is given by:

$$[\Phi(t,0)]\Big|_{(\hat{\underline{x}},\hat{\underline{\lambda}})} = \left[\begin{array}{c:c} \partial\underline{x}(t)/\partial\underline{x}(0) & \partial\underline{x}(t)/\partial\underline{\lambda}(0) \\ \hdashline \partial\underline{\lambda}(t)/\partial\underline{x}(0) & \partial\underline{\lambda}(t)/\partial\underline{\lambda}(0) \end{array}\right]\Bigg|_{(\hat{\underline{x}},\hat{\underline{\lambda}})} \tag{2.26}$$

The evolution of the state transition matrix itself is determined by the differential equation

$$[\dot{\Phi}(t,0)]\Big|_{(\hat{\underline{x}},\hat{\underline{\lambda}})} = [F(t)][\Phi(t,0)]\Big|_{(\hat{\underline{x}},\hat{\underline{\lambda}})} \tag{2.27}$$

where F is given by Eq. (2.12) and $\Phi(0,0)$ is a (2n x 2n) identity matrix. If Eq. (2.27) is integrated simultaneously with $\hat{\underline{x}}$ and $\hat{\underline{\lambda}}$ of step

(a), we can avoid storing $\underline{x}(t)$ and $\hat{\underline{\lambda}}(t)$. We will see that only the upper and lower right corners of $\Phi(T,0)$ are needed in step (c). (The entire Φ matrix is necessary if initial condition continuation [10] methods are used). $\Phi(t,0)$ can also be approximated by direct numerical differentiation [20].

c. The terminal boundary conditions are considered functions of the missing initial co-states. By linearizing about the current estimates of the initial co-states, we obtain the first order corrections $\Delta\underline{\lambda}(0)$ to $\hat{\underline{\lambda}}(0)$ by solving

$$\underline{\psi}(\hat{\underline{x}}(T),\ \hat{\underline{\lambda}}(T)) + \left[\frac{\partial \underline{\psi}(\underline{x}(T),\ \underline{\lambda}(T))}{\partial \underline{\lambda}(0)} \Big|_{(\hat{\underline{x}},\hat{\underline{\lambda}})} \right] \Delta\underline{\lambda}(0) = 0 \qquad (2.28)$$

for $\Delta\underline{\lambda}(0)$, the solution is indicated formally as

$$\Delta\underline{\lambda}(0) = - \left[\frac{\partial \underline{\psi}(\underline{x}(T),\underline{\lambda}(T))}{\partial \underline{\lambda}(0)} \Big|_{(\hat{\underline{x}},\hat{\underline{\lambda}})} \right]^{-1} \underline{\psi}(\hat{\underline{x}}(T),\hat{\underline{\lambda}}(T)) \qquad (2.29)$$

The elements of the partial derivative matrix in Eq. (2.29) can be obtained from $\Phi(T,0)$ and the nominal terminal states and co-states.

d. The previous guesses for the co-state initial conditions are updated by the correction vector $\Delta\underline{\lambda}(0)$ and the steps a through d are repeated until convergence of the initial conditions.

2.4 Polynomial Approximation Methods

Approximation of functions by polynomials has seen widespread use in many engineering and mathematical applications. It has been shown (Weirstrass) that a polynomial of sufficiently high degree can be used

to approximate a continuous single valued function to essentially arbitrary accuracy. However, we occasionally encounter subtle obstacles when constructing algorithms to determine polynomial approximations. The discrete points where interpolating polynomials coincide with the function are often chosen at equal intervals in the desired range. Fox [22] gives an example of polynomial interpolations for a simple function $(1+25x^2)^{-1}$, $-1 \leq x \leq 1$, for which the above choice leads to serious oscillatory errors in between sample points for $|x| \geq .726$, even though their number is increased without bound. This function, however can be fit very accurately if the sample points are chosen non-uniformly such that they coincide with the zeros of a Chebyshev polynomial, or, if one uses equally spaced but heavily redundant sample points (and over-determines the polynomial coefficients by the method of least squares). In other applications, functions may be approximated over small sub-intervals by low order polynomials (e.g. cubic splines), with conditions for continuity imposed at the junctions of adjacent sub-intervals in the range.

In this section, we are interested in approximating functions by a finite polynomial series, over the entire range and extensions of these ideas to the solution ordinary differential equations. As mentioned previously, quasi-linearization is necessary to apply these ideas to nonlinear TPBVPs. We denote each polynomial in the series as a basis function. The vector $\underline{X}(t)$ in the linear TPBVP of Eqs. (2.18-2.20) is approximated to the desired accuracy by

$$\underline{X}(t) = \Phi(t)\underline{A} \tag{2.30}$$

where $\Phi(t)$ = block diagonal $\underline{\phi}^T(t)$

$$\underline{\phi}(t) = [\phi_1(t)\ \phi_2(t)\ ..\ \phi_{NB}(t)]^T$$

$$\underline{A} = [\underline{A}_1^T\ \underline{A}_2^T\ \cdots\ \underline{A}^T{}_{NB}]^T$$

$$\underline{A}_i = [a_{i1}\ a_{i2}\ \cdots\ a_{iNB}]^T$$

$$N = 2n, \text{ the number of differential equations}$$

and NB is the number of basis functions used. Each of the basis functions $\phi_i(t)$ represents an $(i-1)^{th}$ degree polynomial in t, forming a linearly independent, complete set. Each of the a_{ij} represents a coefficient such that the i^{th} variable $X_i(t)$ is represented as

$$X_i(t) = \sum_{j=1}^{NB} a_{ij}\ \phi_j(t) \quad , \quad i = 1,2,\ldots,N. \tag{2.31}$$

The $\phi_i(t)$ are specified functions of time (typically, orthogonal polynomials) and their derivatives often can be obtained through simple recurrence relations. Differentiating Eq. (2.30) we obtain

$$\underline{X}(t) = \dot{\Phi}(t)\underline{A} \tag{2.32}$$

Substituting Eqs. (2.30) and (2.32) into Eq. (2.18), we obtain

$$\dot{\Phi}(t)\underline{A} = [F(t)]\Phi(t)\underline{A} + \underline{D}(t) \tag{2.33}$$

or

$$[\dot{\Phi}(t) - [F(t)]\Phi(t)]\underline{A} = \underline{D}(t) \tag{2.34}$$

or

$$P_1(t)\underline{A} = \underline{D}(t) \tag{2.35}$$

with

$$P_1(t) = \dot{\Phi}(t) - [F(t)]\Phi(t),$$

which is an [N x (N x NB)] known time varying matrix. Equation (2.35) can be evaluated at a number (NS) of sample points at times t_i on (0,T) and thereby establish enough equations to determine the coefficient

vector $\underline{A}$. However, we must ensure satisfaction of boundary conditions. Equations (2.19) and (2.20) are repeated as

$$[U]\underline{X}(0) = \underline{\alpha} \tag{2.36}$$

$$[V]X(T) = \underline{\beta} \tag{2.37}$$

where [U] and [V] are known n x N matrices.

Substituting Eq. (2.30) into Eqs. (2.36) and (2.37) yields the two boundary condition equations

$$P_2\underline{A} = \underline{\alpha} \tag{2.38}$$

$$P_3\underline{A} = \underline{\beta} \tag{2.39}$$

where

$$P_2 = [U]\Phi(0),\ P_3 = [V]\Phi(T). \tag{2.40}$$

Equation (2.35), evaluated at a number (NS) of sample times (t_i) together with the boundary conditions of Eqs. (2.38) and (2.39) yields a merged matrix equation

$$P\underline{A} = \underline{Q} \tag{2.41}$$

where

$$P = \begin{Bmatrix} P_1(t_1) \\ P_1(t_2) \\ \vdots \\ P_1(t_{NS}) \\ P_2 \\ P_3 \end{Bmatrix}, \quad \underline{Q} = \begin{Bmatrix} \underline{D}(t_1) \\ \underline{D}(t_2) \\ \vdots \\ \underline{D}(t_{NS}) \\ \underline{\alpha} \\ \underline{\beta} \end{Bmatrix}$$

Observe, P is an [N x (NS + 1)] x [N x NB] matrix, whereas Q is an [N x (NS + 1)] x 1 vector.

Depending upon the choice of NS, for fixed NB, we solve Eq. (2.41) either by collocation or the method of least squares (i.e., if NS > NB - 1).

Collocation: NS is selected such that P is a square matrix, i.e., NS = NB - 1. Then the coefficients a_{ij} in $\underline{A}$, in principle, are determined uniquely by solving the linear system of Eq. (2.41). Thus the solution $\underline{X}(t)$ can be obtained from Eq. (2.30). This solution satisfies the differential equation only at the sample points; the boundary conditions are satisfied exactly. As NB is increased sufficiently, the average error at intermediate points typically tends to zero.

Method of Least Squares: If NS is selected such that NS > (NB - 1) we determine the $\underline{A}$ solution using a least squares criterion. This overdetermined solution tends to be smoother and is useful if oscillatory errors are encountered. If the simple least squares method is used, the computed solution matches the actual solution at none of the sample points and boundary conditions will not be satisfied exactly, but the square error is uniformly small throughout the range. The method of constrained least squares [23] can be used to enforce exact satisfaction of the boundary conditions.

For nonlinear problems, instead of obtaining $\underline{A}$, we obtain corrections $\Delta\underline{A}$ to these (the initial a_{ij} are determined easily, since we select nominal profiles $\hat{\underline{X}}(t)$). The correction vector $\Delta\underline{X}(t)$ to $\hat{\underline{X}}(t)$ is expressed as:

$$\Delta\underline{X}(t) = \Phi(T)\Delta\underline{A} \tag{2.42}$$

and the updated nominal solution is

$$\underline{X}(t) = \Phi(t)\{\underline{A} + \Delta\underline{A}\}.$$

Since the starting solution is typically not very accurate, we may want to restrict the number of basis functions (NB) to a smaller number until the final stages of the solution process. As more accurate solutions are obtained, NB can be increased in an adaptive fashion. The linearized TPBVP may require more than one correction to converge accurately, for each NB.

The basis functions can be chosen from any linearly independent, complete set of polynomials, e.g., Chebyshev, Legendre, as well as transcendental basis functions. We consider Chebyshev polynomials in the following examples. There are two popular choices for selecting the sample intervals; uniform intervals are convenient but are not optimum from a curve fitting view point, and nonuniform spacing based on the zeros of the polynomials used in the series though better, might not be convenient for table lookup and interpolation. For Chebyshev polynomials, the zeros occur at higher frequencies near the boundaries (compared to the middle of the normalized time range (-1, 1) over which the polynomials are defined). Hence, such interval spacing is better suited to match the true solution in the vicinity of the boundaries.

Another class of methods which exploits the orthogonality of the basis functions is the weighted residual methods (e.g., Galerkin's method), see Meirovitch [24]. For our problems, we would need to express elements of [F (t)] and $\underline{D}$ (t) in Chebyshev series, which would greatly increase the storage requirements. Recurrence relations for Chebyshev polynomials can be found in [22].

Quasi-linearization and the method of differential corrections are both second-order gradient methods. Since both are realizations of a Newton-Raphson method, they converge quadratically but are sensitive to the guesses of profiles $\hat{\underline{x}}(t)$ or missing initial conditions on $\hat{\underline{\lambda}}(t)$. Thus, they need good estimates to converge reliably to the actual solution. The method of particular solutions and polynomial approximation on the other hand, are directly applicable to linear TPBVPs only. The method of polynomial approximation is well suited for lower order problems which cannot be solved by methods using numerical integration (e.g., extremely stiff but low-dimensional systems), for large systems, the drawback is essentially due to the need for the solution of large non-sparse linear systems. For problems which are sensitive to initial conditions, the method of particular solutions has been found more attractive (it converges from poor starting estimates for a wider class of problems) than shooting techniques which iterate using integrations of the parent non-linear equations.

2.5 CONTINUATION

Continuation methods (or, Homotopy methods) are a family of numerical procedures which augments the capabilities of all of the above methods for solving numerically sensitive TPBVPs by decreasing the reliance upon a good initial guess. Discussions and applications can be found in [10,14]. In essence, a continuous one parameter (α) family of problems is introduced. The family is constructed so that it degenerates for ($\alpha = 0$) to a problem whose solution is available (or can be determined analytically); and for $\alpha = 1$, it reduces to the problem

whose solution is desired. By sweeping α, we can define a large number (if required) of neighboring TPBVPs. By extrapolating from neighboring α solutions having converged values for the missing boundary conditions, the iteration for an intermediate α solution can be initiated with "arbitrarily close" starting estimates. Except for local singular events (e.g., bifurcation points), this approach can very nearly guarantee convergence. The method of neighboring extremals [20] belongs to this class of methods; it utilizes the shooting method of differential corrections with a boundary condition continuation method. The method of modified quasi-linearization [25] has an effect similar to continuation. The boundary condition relaxation method of Junkins and Turner [10] is a form of continuation.

2.6 OTHER METHODS

Other methods for stiff and numerically sensitive problems generally solve the TPBVP by converting it in to a multipoint boundary value problem; i.e., a finite number (N) of TPBVP's are solved over small intervals $[t_1, t_2]$, ..., $[t_{N-1}, T]$ and the solutions are matched at the junctions by continuity conditions. This, in effect, restricts the growth and decay of the solutions over each sub-interval. See for example the works of Ojika et al. [26], Graney [27], Deuflhard et al. [28], Orava and Lautala [29], and Miele et al. [30].

2.7 TWO EXAMPLES SOLVED BY THREE METHODS

Example 2.1

This linear TPBVP [26] is selected to demonstrate the effect of stiffness:

$$\begin{Bmatrix} \dot{x}_1 \\ \dot{x}_2 \end{Bmatrix} = \begin{bmatrix} 1 & 1 \\ k^2 & 1 \end{bmatrix} \begin{Bmatrix} x_1 \\ x_2 \end{Bmatrix} , \; x_1(0) = 1, \; x_2(T) = 0 \tag{2.43}$$

where k is positive and the eigenvalues of the system matrix are $1 \pm k$. The problem obviously has a stiff behavior when k is large. The analytical solution is:

$$x_1(t) = \frac{1}{2}\{e^{(1+k)t} + e^{(1-k)t}\} - \frac{1}{2}\{e^{(1+k)T} - e^{(1-k)T}\}\{e^{(1+k)t} - e^{(1-k)t}\}/\{e^{(1+k)T} + e^{(1-k)T}\} \tag{2.44}$$

$$x_2(t) = \frac{k}{2}\{e^{(1+k)t} - e^{(1-k)t}\} - \frac{k}{2}\{e^{(1+k)T} - e^{(1-k)T}\}\{e^{(1+k)t} + e^{(1-k)t}\}/\{e^{(1+k)T} + e^{(1-k)T}\} \tag{2.45}$$

It is easy to see that the missing initial condition is $x_2(0) = -5$, for $k = 5$ and $T = 5$. The analytical solution, the solution obtained by numerical integration with known initial conditions, and the solution by the method of particular solutions (Section 2.3.1) at the initial and final times are tabulated in Table 2.1. It should be noted that this deceptive problem is well-known, and most challenging, from the viewpoint of obtaining accurate numerical solutions over long time intervals.

As can be seen from Table 2.1, the direct Runge-Kutta integration and the Method of Particular Solutions produce results which agree with the analytical solution up to seven decimal figures at 2.5 seconds,

though they diverge considerably later on. The missing initial condition is, however, obtained correctly by the method of particular solutions. The Runge-Kutta solution is given the correct initial condition to illustrate the difficulty of forward integration. These errors do not decrease for 16 digit precision if step size is decreased. The Chebyshev polynomial method (Section 2.4) is now applied to this problem. The sample points are selected in two ways, one with equal itnervals and the other corresponding to the zeros of a Chebyshev polynomial.

The Chebyshev polynomial of the first kind is given by:

$$T_k(\tau) = \cos(k \cos^{-1}(\tau)) \quad , \quad -1 \leq \tau \leq 1 \tag{2.46}$$

where k is the degree of the polynomial and τ is given by

$$\tau = \frac{2t}{T} - 1 \tag{2.47}$$

The differentials with respect to τ are related to those with respect to t by

$$\frac{d}{d\tau}( ) = \frac{d}{dt}( ) \frac{dt}{d\tau} = \frac{T}{2} \frac{d}{dt}( ) \tag{2.48}$$

The zeros of the Chebyshev polynomial of degrees NS-1 are

$$\tau_i = \cos \frac{(i-1)\pi}{NS-1} \quad , \quad i = 1,\ldots,NS \tag{2.49}$$

The solution for $x_i(t)$ is obtained as discussed in Section 2.4. The effects of NB and NS on the solution, as well as the effects of uniform versus cosine sampling, are summarized in Table 2.2.

As can be seen, the solution by the method of collocation with cosine sampling is closer to the analytical solution at the boundary though it is slightly in error in the middle of the range (after about 2.5 seconds). With uniform samples, although the solution matches the analytical one closely up to 2.5 seconds and more, there is a larger error near the final boundary. It can also be seen (from the densely calculated solution) that the method of least squares has less average error, especially with cosine sampling.

The convergence of the Chebyshev series can be observed from the rate at which the coefficients a_{ij} decrease. For NS = 29 and NB = 30, the coefficients are given in Table 2.3. These results suggest that polynomial approximation and collocation methods are advantageous for stiff systems. However, as mentioned earlier, the large linear systems encountered for high dimensioned systems limits this approach to problems of modest dimensionality. Table 2.4 presents the more detailed solutions obtained by collocation and the method of particular solutions, the trajectories $x_1(t)$ and $x_2(t)$ are shown in Fig. 2.1. As is evident from Table 2.4, the Chebyshev/collocation numerical solution, for NB = 30, NS = 29, converged accurately to the analytical solution, whereas the method of particular solutions diverges after t = 3 sec.

TABLE 2.1

RUNGE-KUTTA AND METHOD OF PARTICULAR SOLUTIONS APPLIED TO EXAMPLE 2.1

TIME	ANALYTICAL SOLUTION		DIRECT INTEGRAITON 4 CYC RUNGE-KUTTA STEP SIZE .001		METHOD OF PARTICULAR SOLUTION (4 CYC RUNGE-KUTTA) STEP SIZE .001	
t (sec)	x_1	x_2	x_1	x_2	x_1	x_2
0	1.0	-5.0	1.0	-5.0	1.0	-5.0
2.5	.45400E-4	-.22700E-3	.45403E-4	-.22698E-3	.45393E-4	-.22708E-3
5	.41223E-8	0.0	.11329E-1	.56643E-1	-.23438E-1	-.39063E-2

TABLE 2.2

CHEBYSHEV POLYNOMIAL SOLUTIONS OF EXAMPLE 2.1

TIME	UNIFORM SAMPLING NS=21, NB=22		COSINE SAMPLING NS=21, NB=22		UNIFORM SAMPLING NS=31, NB=22		COSINE SAMPLING NS=31, NB=22	
(t sec)	x_1	x_2	x_1	x_2	x_1	x_2	x_1	x_2
0.0	1.0	-5.0	1.0	-5.0	1.0	-5.0	1.0	-5.0
2.5	.45400E-4	-.22700E-3	.45402E-4	-.22701E-3	.45400E-4	-.22700E-3	.45401E-4	-.22701E-3
5.0	3.79 E-7	5.59 E-16	4.09 E-9	2.30 E-16	1.08 E-8	-1.12 E-16	3.96 E-9	-1.48 E-16

TABLE 2.3

CHEBYSHEV COEFFICIENTS FOR EXAMPLE 2.1

i	a_{1i}	a_{2i}
1	.12783	- .63917
2	.24253	-1.21263
3	.20716	-1.03551
4	.15966	- .79830
10	.47506E-2	- .23753E-1
15	.31159E-4	- .15580E-3
20	.48000E-7	- .24000E-6
25	.23274E-10	- .11638E-9
30	.29756E-14	- .20507E-13

TABLE 2.4

TRAJECTORIES FOR EXAMPLE 2.1

TIME t (sec)	ANALYTICAL SOLUTION [14]		COLLOCATION NS=29, NB=30 COSINE SAMPLING		METHOD OF PARTICULAR SOLUTIONS	
	x_1	x_2	x_1	x_2	x_1	x_2
0	1.0	-5.0	1.0	-5.0	1.0	-5.0
.5	.13534E0	-.67668E0	.13534E0	-.67668E0	.13534E0	-.67668E0
1.0	.18316E-1	-.91578E-1	.18316E-1	-.91578E-1	.18316E-1	-.91578E-1
1.5	.24788E-2	-.12394E-1	.24788E-2	-.12394E-1	.24788E-2	-.12394E-1
2.0	.33546E-3	-.16773E-2	.33546E-3	-.16773E-2	.33546E-3	-.16773E-2
2.5	.45400E-4	-.22700E-3	.45400E-4	-.22700E-3	.45394E-4	-.22708E-3
3.0	.61442E-5	-.30721E-4	.61442E-5	-.30721E-4	.60275E-5	-.31888E-4
3.5	.85153E-6	-.41576E-5	.83153E-6	-.41576E-5	-.59605E-5	-.26703E-4
4.0	.11254E-6	-.56265E-6	.11254E-6	-.56265E-6	-.21362E-3	.12207E-3
4.5	.15333E-7	-.75637E-7	.15333E-7	-.75637E-7	-.34180E-2	.21973E-2
5.0	.41223E-8	0.0	.41223E-8	.151E-15	-.23438E-1	-.39063E-2

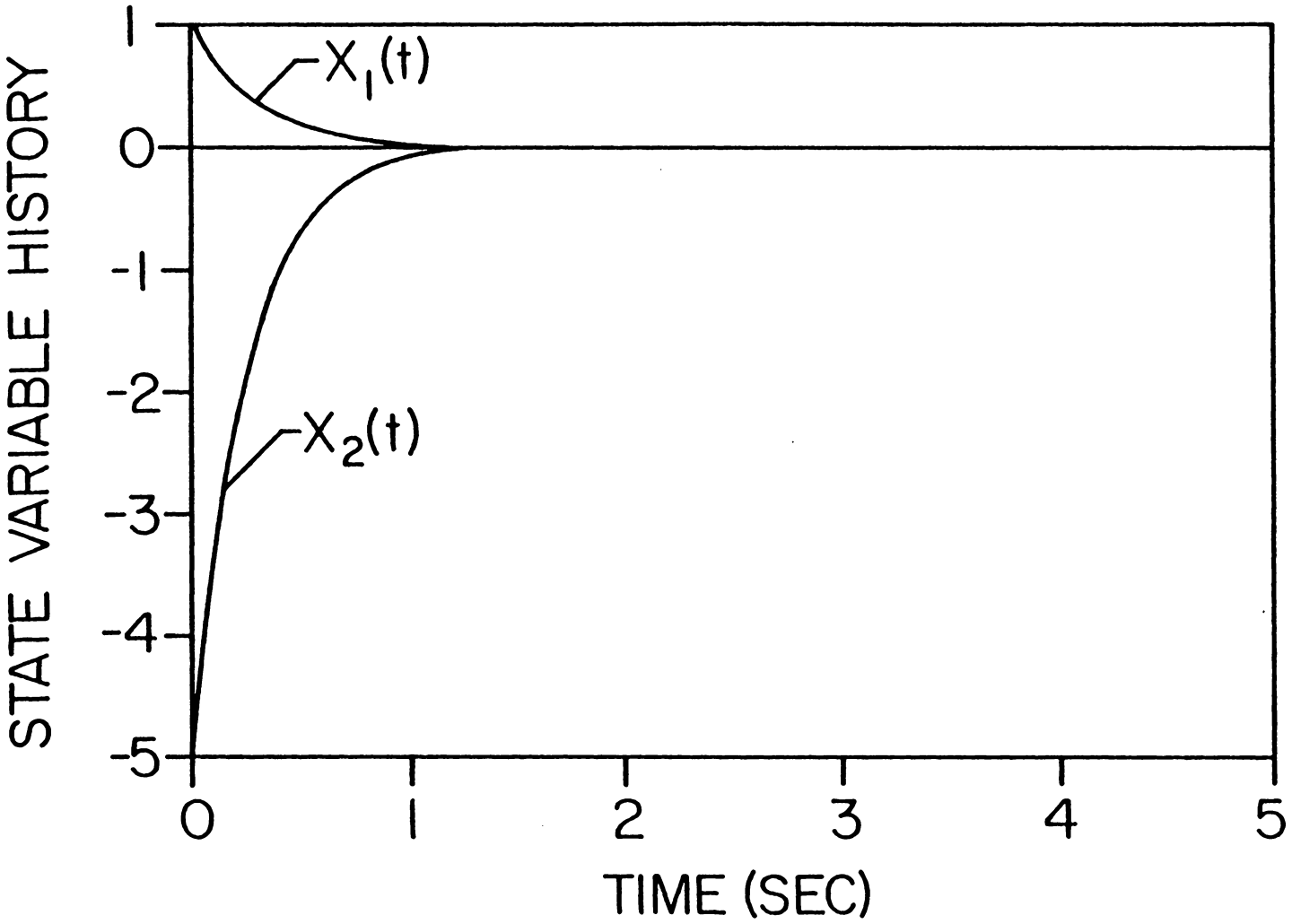

Fig. 2.1 State variable history for Example 2.1.

Example 2.2

In this example, we consider optimal detumble maneuvers of a rigid asymmetric spacecraft. The Euler's equations for the angular velocities ω_i of the spacecraft are given by

$$\begin{aligned} \dot{\omega}_1 &= - J_1 \omega_2 \omega_3 + L_1/I_1 \\ \dot{\omega}_2 &= - J_2 \omega_3 \omega_1 + L_2/I_2 \\ \dot{\omega}_3 &= - J_3 \omega_1 \omega_2 + L_3/I_3 \end{aligned} \tag{2.50}$$

where L_i are the control torques, and (I_1, I_2, I_3), the spacecraft principal inertias, and $J_1 = (I_3 - I_2)/I_1$, $J_2 = (I_1 - I_3)/I_2$, $J_3 = (I_2 - I_1)/I_3$, the inertia difference ratios.

The performance index based on control torque histories is selected as

$$J = \frac{1}{2} \int_0^T (L_1^2 + L_2^2 + L_3^2) dt \tag{2.51}$$

We seek the continuous unbounded controls $L_i(t)$ which minimize J subject to Eq. (2.50) with specified initial and final boundary conditions on the $\omega_i(t)$. Application of Pontryagin's principle (Appendix A) leads to a TPBVP constituted by the following six state and co-state differential equations.

$$\begin{aligned} \dot{\omega}_1 &= - J_1 \omega_2 \omega_3 - \lambda_1/I_1^2 \quad , \quad \dot{\lambda}_1 = J_2 \omega_3 \lambda_2 + J_3 \omega_2 \lambda_3 \quad , \quad L_i = - \lambda_i/I_i \\ \dot{\omega}_2 &= - J_2 \omega_3 \omega_1 - \lambda_2/I_2^2 \quad , \quad \dot{\lambda}_2 = J_1 \omega_3 \lambda_1 + J_3 \omega_1 \lambda_3 \\ \dot{\omega}_3 &= - J_3 \omega_1 \omega_2 - \lambda_3/I_3^2 \quad , \quad \dot{\lambda}_3 = J_1 \omega_2 \lambda_1 + J_2 \omega_1 \lambda_2 \end{aligned} \tag{2.52}$$

We see that we have six nonlinear, gyroscopically coupled differential equations.

Arbitrary initial angular velocity boundary conditions can be prescribed; the terminal angular velocities are to be driven to zero. Hence, for the system of six equations, we have six state boundary conditions but no conditions on the co-states are specified. We choose the state boundary conditions as

$$\omega_1(0) = 0.01 \text{ r/s}, \ \omega_2(0) = 0.005 \text{ r/s}, \ \omega_3(0) = 0.001 \text{ r/s},$$
$$\omega_1(T) = \omega_2(T) = \omega_3(T) = 0, \ T = 100 \text{ sec},$$

and inertias as

$$I_1 = 86.24 \text{ kg m}^2, \ I_2 = 85.07 \text{ kg m}^2, \ I_3 = 113.59 \text{ kg m}^2.$$

We first apply the polynomial approximation (collocation) method of Section 2.4, using Chebyshev polynomials as basis functions. Since the initial angular velocities are low and the final time (100 sec) is relatively long, we expect low torque levels. One choice for the nominal solution is obtained by integrating Eq. (2.52) with the prescribed initial states and zeros for the initial co-states. On the other hand, it is more convenient for the Chebyshev method (since the determination of coefficients is near-trivial) to use a linear approximation for the states, between the two boundaries; the co-states are again assumed to be zero throughout. Then the Chebyshev coefficients for the linear approximations are

$$\begin{aligned} a_{i1} &= (\omega_i(0) + \omega_i(T))/2 \\ a_{i2} &= (-\omega_i(0) + \omega_i(T))/2 \end{aligned} \qquad i = 1,2,3 \qquad (2.53)$$

and the rest of the coefficients are zero.

The Jacobian matrix F required for this nonlinear problem is obtained by differentiation of the differential Eq. (2.52) as

$$F = \begin{bmatrix} 0 & -J_1\omega_3 & -J_1\omega_2 & -1/I_1^2 & 0 & 0 \\ -J_2\omega_3 & 0 & -J_2\omega_1 & 0 & -1/I_2^2 & 0 \\ -J_3\omega_2 & -J_3\omega_1 & 0 & 0 & 0 & -1/I_3^2 \\ 0 & J_3\lambda_3 & J_2\lambda_2 & 0 & J_2\omega_3 & J_3\omega_2 \\ J_3\lambda_3 & 0 & J_1\lambda_1 & J_1\omega_3 & 0 & J_3\omega_1 \\ J_2\lambda_2 & J_1\lambda_1 & 0 & J_1\omega_2 & J_2\omega_1 & 0 \end{bmatrix} \tag{2.54}$$

The solutions obtained by three different methods agreed to at least seven figures. The missing initial conditions are found to be

$$\lambda_1(0) = 0.74373376$$

$$\lambda_2(0) = 0.361845245$$

$$\lambda_3(0) = 0.129026881$$

We find that the method of collocation with Chebyshev sample points needs only seven basis functions to represent the solutions to this accuracy. Figure 2.2 shows the optimal trajectories and control torques. The number of iterations and the CPU time on the IBM 370/3032 computer are tabulated for each the three methods in Table 2.5.

2.8 Concluding Remarks

The obvious conclusions one can draw from these simple examples is that the Chebyshev method is superior to the other methods, for these two examples, but this conclusion holds only for low order problems and especially problems whose solutions are accurately representable by a small number of the chosen basis functions. For higher order problems, we find that computer storage and solution of large linear systems become more serious problems and the other two methods prove more widely applicable.

The present chapter develops the formulations and illustrates typical numerical results for three commonly used procedures for solving TPBVPs. These results are generated and extended for solving problems of higher dimensionality in the subsequent chapters.

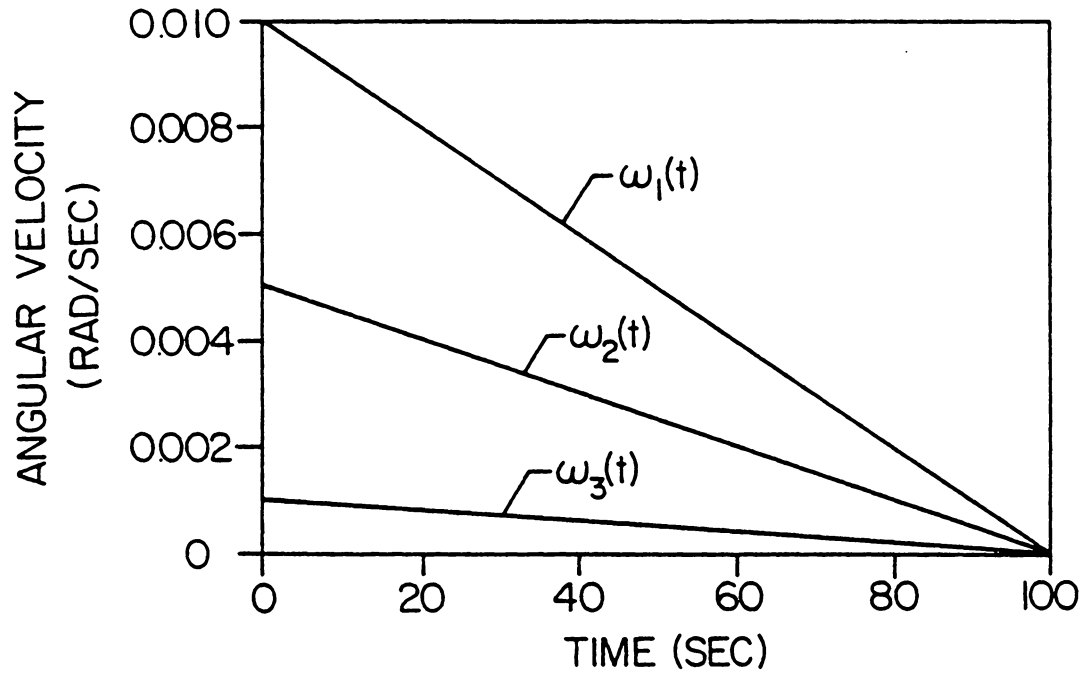

Fig. 2.2 (a) Angular velocity components for Example 2.2.

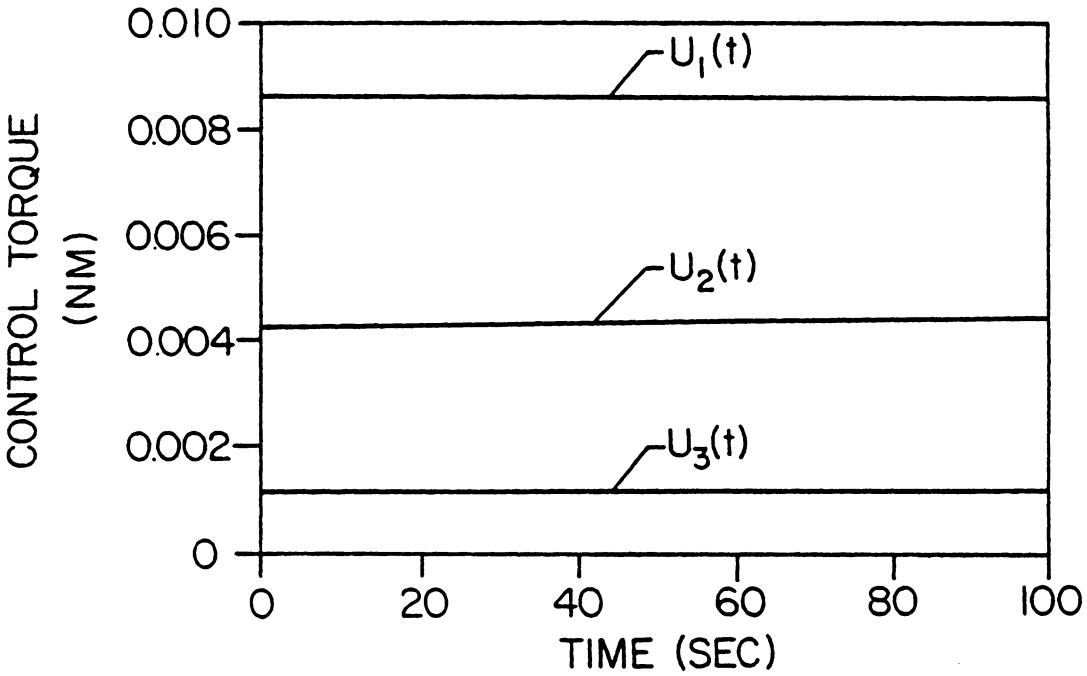

Fig. 2.2 (b) Optimal control torques for Example 2.2.

TABLE 2.5

COMPUTATIONAL SUMMARY FOR THREE SOLUTIONS OF EXAMPLE 2.2

	Method of Particular Solutions (Section 2.4)	Differential Correction Shooting Technique (Section 2.5)	Chebyshev Polynomial Collocation (Cosine Sampling) (Section 2.6)
CPU TIME (SEC)	16	11	8
# OF ITERATIONS	5	5	4

CHAPTER III

OPTIMAL ATTITUDE MANEUVERS WITH EXTERNAL TORQUES

A detumble maneuver (Example 2.2) for an unsymmetric spacecraft was presented in Chapter II. A more general maneuver which not only controls the angular velocity of the spacecraft but also performs desired reorientation using external torques, is considered in this chapter.

3.1 SPACECRAFT ORIENTATION AND ROTATIONAL KINEMATICS

The orientation of an arbitrary body-fixed frame $\{\hat{\underline{b}}\}$ with respect to an arbitrary intertial frame $\{\hat{\underline{n}}\}$ is given by

$$\{\hat{\underline{b}}\} = [C]\{\hat{\underline{n}}\} \tag{3.1}$$

Although the direction cosine matrix [C] is commonly parameterized in terms of a set of three Euler angles, it is advantageous (Morton et al. [31]) to use the set of four Euler parameters $(\beta_0,\beta_1,\beta_2,\beta_3)$ instead, as

$$[C] = [C(\beta)] = \begin{bmatrix} \beta_0^2+\beta_1^2-\beta_2^2-\beta_3^2 & 2(\beta_1\beta_2+\beta_0\beta_3) & 2(\beta_1\beta_3-\beta_0\beta_2) \\ 2(\beta_1\beta_2-\beta_0\beta_3) & \beta_0^2-\beta_1^2+\beta_2^2-\beta_3^2 & 2(\beta_2\beta_3+\beta_0\beta_1) \\ 2(\beta_1\beta_3+\beta_0\beta_2) & 2(\beta_2\beta_3-\beta_0\beta_1) & \beta_0^2-\beta_1^2-\beta_2^2+\beta_3^2 \end{bmatrix} \tag{3.2}$$

The Euler parameters have a geometrical interpretation in terms of Euler's theorem which states that a completely general rotation of a rigid body can be accomplished by a single rotation (through the principal angle, ϕ_{nb}) about a line (the principal line, $\hat{\underline{\ell}}_{nb}$) which is fixed relative to both the arbitrary body-fixed axes and the inertial reference frame (see Fig. 3.1). The Euler parameters are related to the direction cosines $(\ell_{nb1},\ell_{nb2},\ell_{nb3})$ of $\hat{\underline{\ell}}_{nb}$ and ϕ_{nb} as

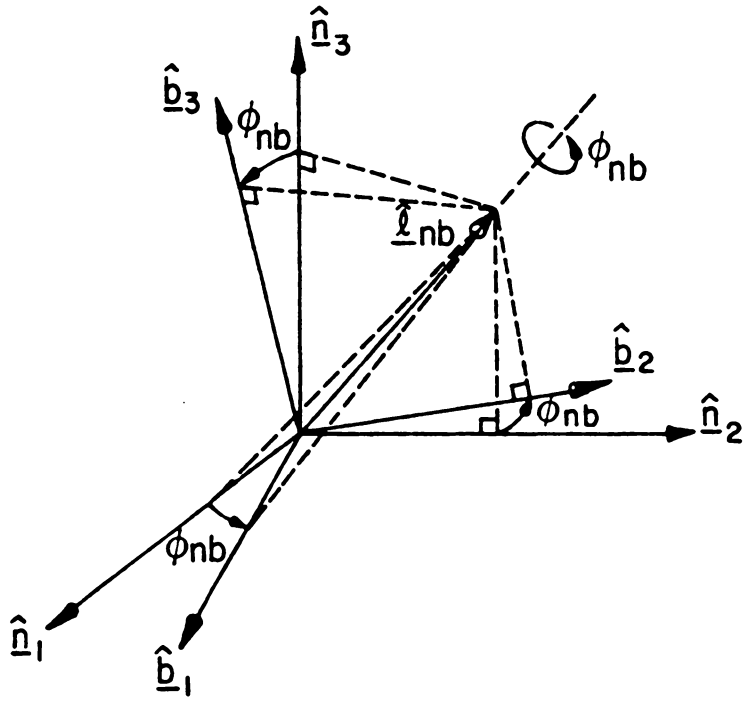

Fig. 3.1 Principal rotation ϕ_{nb} about $\hat{\ell}_{nb}$ defining orientation of $\{\hat{b}\}$ relative to $\{\hat{n}\}$.

$$\beta_0 = \cos(\phi_{nb}/2),$$

$$\beta_i = \ell_{nbi} \sin(\phi_{nb}/2) \quad , \quad i = 1,2,3. \tag{3.3}$$

Thus the Euler parameters are once-redundant due to the constraint

$$\sum_{i=0}^{3} \beta_i^2 = 1 \tag{3.4}$$

The Euler parameter differential equations can be written (Whittaker [32]) as

$$\dot{\underline{\beta}} = [G(\omega)]\underline{\beta} \tag{3.5}$$

where

$$[G(\omega)] = \frac{1}{2}\begin{bmatrix} 0 & -\omega_1 & -\omega_2 & -\omega_3 \\ \omega_1 & 0 & \omega_3 & -\omega_2 \\ \omega_2 & -\omega_3 & 0 & \omega_1 \\ \omega_3 & \omega_2 & -\omega_1 & 0 \end{bmatrix} \tag{3.6}$$

and ω_i are the components of the angular velocity of $\{\hat{\underline{b}}\}$ with respect to $\{\hat{\underline{n}}\}$ expressed in the $\{\hat{\underline{b}}\}$ frame. Notice that the coefficient matrix [G] is skew symmetric, so that

$$[G] = -[G]^T$$

3.2 SPACECRAFT DYNAMICS

Euler's equations for rotational motion of a rigid spacecraft in body-fixed principal axes system, Eq. (2.50) are re-written as follows:

$$\begin{aligned} \dot{\omega}_1 &= -J_1\omega_2\omega_3 + L_1/I_1 \\ \dot{\omega}_2 &= -J_2\omega_1\omega_3 + L_2/I_2 \\ \dot{\omega}_3 &= -J_3\omega_1\omega_2 + L_3/I_3 \end{aligned} \tag{3.8}$$

3.3 OPTIMAL MANEUVERS

The four Euler parameters β_i and the three angular velocities ω_j, together describe the orientation (attitude) and dynamics of the spacecraft completely and hence are treated as state variables. Orientations prescribed in terms of any of the twelve sets of Euler angles can be transformed to Euler parameters by transformations given by Morton [33].

Maneuvers are performed to transfer the spacecraft from its initial state to prescribed final state at time, T, using external control torques L_1, L_2, and L_3. The performance index to be minimized is selected as

$$J = \frac{1}{2} \int_0^T \left[\sum_{i=1}^{3} L_i^2(t) \right] dt \tag{3.9}$$

The necessary conditions for optimal maneuvers are derived via the Pontryagin's principle (Appendix A). The Hamiltonian for the system given by Eqs. (3.5) and (3.8), and the performance index of Eq. (3.9) is written as

$$H = \frac{1}{2} (L_1^2 + L_2^2 + L_3^2) + \underline{\gamma}^T \dot{\underline{\beta}} + \underline{\lambda}^T \dot{\underline{\omega}} \tag{3.10}$$

where $\underline{\gamma}$ and $\underline{\lambda}$ are seven co-states or Lagrange multipliers. The controls L_i are required to satisfy the optimality condition:

$$\frac{\partial H}{\partial L_i} = 0 = L_i + \lambda_i / I_i$$

or

$$L_i = - \lambda_i / I_i \tag{3.11}$$

The co-state differential equations are given by

$$\dot{\underline{\gamma}} = -\frac{\partial H}{\partial \underline{\beta}}$$

and (3.12)

$$\dot{\underline{\lambda}} = -\frac{\partial H}{\partial \underline{\omega}}$$

In their final form, the state and co-state equations are given below

State equations:

$$\dot{\underline{\beta}} = [G(\omega)]\underline{\beta} \tag{3.13}$$

$$\begin{aligned}\dot{\omega}_1 &= -J_1\omega_2\omega_3 - \lambda_1/I_1^2 \\ \dot{\omega}_2 &= -J_2\omega_1\omega_3 - \lambda_2/I_2^2 \\ \dot{\omega}_3 &= -J_3\omega_1\omega_2 - \lambda_3/I_3^2\end{aligned} \tag{3.14}$$

Co-state equations:

$$\dot{\underline{\gamma}} = [G(\omega)]\underline{\gamma} \tag{3.15}$$

$$\dot{\underline{\lambda}} = \begin{bmatrix} 0 & J_3\lambda_3 & J_2\lambda_2 \\ J_3\lambda_3 & 0 & J_1\lambda_1 \\ J_2\lambda_2 & J_1\lambda_1 & 0 \end{bmatrix} \begin{Bmatrix} \omega_1 \\ \omega_2 \\ \omega_3 \end{Bmatrix} + \frac{1}{2} \begin{bmatrix} \beta_1 & -\beta_0 & -\beta_3 & \beta_2 \\ \beta_2 & \beta_3 & -\beta_0 & -\beta_1 \\ \beta_3 & -\beta_2 & \beta_1 & -\beta_0 \end{bmatrix} \begin{Bmatrix} \gamma_0 \\ \gamma_1 \\ \gamma_2 \\ \gamma_3 \end{Bmatrix}$$

(3.16)

Boundary conditions at the initial and final times are specified on $\underline{\beta}$ and $\underline{\omega}$. No boundary conditions are available on $\underline{\gamma}$ and $\underline{\lambda}$; their initial (or final) boundary conditions can only be determined through solution of the TPBVP.

3.4 SOLUTION OF THE TPBVP

Analytical closed form solutions to the TPBVP have been presented in [10] for special case boundary conditions corresponding to single axis maneuvers about any one of the three principal axes. Such boundary conditions, corresponding to the maneuver about the i^{th} axis are as follows:

$$\beta_0(0) = \beta_{00} \qquad \beta_0(T) = \beta_{0T}$$
$$\beta_i(0) = \beta_{i0} \qquad \beta_i(T) = \beta_{iT}$$
$$\beta_j(0) = 0 \qquad \beta_j(T) = 0 \quad , \quad j \neq 0,i$$
$$\omega_i(0) = \omega_{i0} \qquad \omega_i(T) = \omega_{iT}$$
$$\omega_j(0) = 0 \qquad \omega_j(T) = 0 \quad , \quad j \neq i$$

It is shown in [10] that for single-axis solutions, the missing $\underline{\gamma}$ initial conditions are not unique; one particular solution (the so called minimum norm solution) is such that $\|\underline{\gamma}\| = B$, is a minimum. The nonuniqueness of $\underline{\gamma}(0)$ is a direct consequence of the fact that we have elected to use a once-redundant parameterization of spacecraft orientation (i.e., the Euler parameters). Using this closed form solution [10], the more general three-axis maneuvers are computed using a differential corrections scheme in conjunction with a boundary condition continuation process. As in the case of single-axis maneuvers, the minimum norm solution is obtained at each continuation step. The rigorous minimization of $\|\underline{\gamma}\|$ complicates the algorithm to some extent.

3.4.1 ON THE MINIMUM NORM SOLUTION

Some properties of the state and co-state equations (3.12-3.15) along with a result on the minimum norm solution are presented in this subsection.

Note the following integrals of the state and co-state differential equations (3.13) and (3.15)

1. $\underline{\beta}^T(t)\underline{\beta}(t) = 1$ (3.17)

which follows from the definition of the Euler parameters (Eq. (3.3)).

2. $\underline{\gamma}^T(t)\underline{\gamma}(t) = \text{constant} = B^2$ (3.18)

as $\underline{\gamma}(t)$ satisfies a skew-symmetric differential equation (3.15) similar to Eq. (3.13).

3. $\underline{\beta}^T(t)\underline{\gamma}(t) = \text{constant} = C$ (3.19)

This can be shown by differentiating $\underline{\beta}^T(t)\underline{\gamma}(t)$, to obtain

$$\frac{d}{dt}[\underline{\beta}^T(t)\underline{\gamma}(t)] = \dot{\underline{\beta}}^T(t)\underline{\gamma}(t) + \underline{\beta}^T(t)\dot{\underline{\gamma}}(t) \tag{3.20}$$

Eliminating $\dot{\underline{\beta}}^T$ and $\dot{\underline{\gamma}}(t)$ through Eqs. (3.13) and (3.15) respectively, results in

$$\frac{d}{dt}[\underline{\beta}^T(t)\underline{\gamma}(t)] = \underline{\beta}^T[G^T]\underline{\gamma} + \underline{\beta}^T[G]\underline{\gamma} \tag{3.21}$$

Using Eq. (3.7) in Eq. (3.21) we obtain

$$\frac{d}{dt}[\underline{\beta}^T(t)\underline{\gamma}(t)] = 0 \tag{3.22}$$

and hence $\underline{\beta}^T(t)\underline{\gamma}(t) = \text{constant} = C$.

Admissible Euler Parameter Co-States:

Although an infinite number of $\underline{\gamma}(0)$ could satisfy the necessary conditions for optimality, they are not totally arbitrary. As a simple example let us consider $\underline{\gamma}(t) = a\,\underline{\beta}(t)$, where a is an arbitrary costant. Then

$$\underline{\gamma}^T\dot{\underline{\beta}} = a\underline{\beta}^T\dot{\beta} = \frac{1}{2}\,a\,\frac{d}{dt}\,(\underline{\beta}^T\underline{\beta}) = \frac{1}{2}\,a\,\frac{d}{dt}\,(1) = 0$$

Observe that this choice for $\underline{\gamma}(t)$ decouples the attitude and dynamics in the Hamiltonian (3.10), and only the angular velocity of the spacecraft can be controlled; arbitrary terminal attitude specifications cannot be met. Hence

$$\underline{\gamma}(t) \neq a\underline{\beta}(t) \tag{3.23}$$

Since all the admissible $\underline{\gamma}(t)$ produce the same control $\underline{L}(t)$, which in turn are dictated by $\underline{\lambda}(t)$, the differential equations for $\lambda_i(t)$ should be invariant with respesct to these $\underline{\gamma}(t)$. Since the problem at hand is nonlinear and a general analytical solution does not exist, we cannot quantitatively determine the nature of $\underline{\gamma}(t)$ without numerical means. Hence to gain qualitative insight into the problem, we assume that an admissible numerical solution $\underline{\gamma}(t)$ has been obtained. Let

$$\underline{\gamma}_a(t) = \underline{\gamma}(t) + \delta\underline{\gamma}(t) \tag{3.24}$$

denote the admissible neighboring co-state vector and $\delta\underline{\gamma}(t)$ be admissible variations. To identify the nature of the admissible variations we substitute Eq. (3.24) into Eq. (3.16) to obtain

$$\begin{bmatrix} \beta_1 & -\beta_1 & -\beta_3 & \beta_2 \\ \beta_2 & \beta_3 & -\beta_o & -\beta_1 \\ \beta_3 & -\beta_2 & \beta_1 & -\beta_o \end{bmatrix} \delta\underline{\gamma}(t) = \underline{0} \tag{3.25}$$

An additional constraint is obtained by substituting Eq. (3.24) into Eq. (3.19) as

$$\underline{\beta}^T(t)[\underline{\gamma}(t) + \delta\underline{\gamma}(t)] = C_a \tag{3.26}$$

where C_a is an arbitrary constant, dependent on $\underline{\gamma}_a(t)$, or

$$\beta^T(t)\delta\underline{\gamma}(t) = C_a - C \tag{3.27}$$

Combining Eqs. (3.25) and (3.27) we obtain

$$\begin{bmatrix} \beta_1 & -\beta_o & -\beta_3 & \beta_2 \\ \beta_2 & \beta_3 & -\beta_o & -\beta_1 \\ \beta_3 & -\beta_2 & \beta_1 & -\beta_o \\ \beta_o & \beta_1 & \beta_2 & \beta_3 \end{bmatrix} \delta\underline{\gamma}(t) = \begin{Bmatrix} 0 \\ 0 \\ 0 \\ C_a - C \end{Bmatrix} \tag{3.28}$$

Since the coefficient matrix is orthogonal, the solution to the above equation can be written as

$$\delta\underline{\gamma}(t) = (C_a - C)\underline{\beta}(t) = \alpha_a\underline{\beta}(t) \tag{3.29}$$

where

$$\alpha_a = C_a - C$$

Hence we have the family of admissible attitude co-states given by

$$\underline{\gamma}_a(t) = \underline{\gamma}(t) + \alpha_a\underline{\beta}(t) \tag{3.30}$$

It is seen from Eqs. (3.30) and (3.23) that $\underline{\gamma}(t)$ is never zero.

Of particular interest is the solution with $\underline{\gamma}_m(t)$ $\{\gamma: \|\gamma^T\gamma\| = B^2$, is a minimum$\}$.

In order to perform a minimization we form the inner product

$$\begin{aligned} \underline{\gamma}_a^T(t)\underline{\gamma}_a(t) &= \underline{\gamma}^T(t)\underline{\gamma}(t) + 2\alpha_a\underline{\gamma}^T\underline{\beta}(t) + \alpha_a^2 \\ &= B^2 + 2\alpha_a C + \alpha_a^2 \end{aligned} \tag{3.31}$$

As α_a is the parameter in Eq. (3.31) it is easy to see that

$$\alpha_m = -C \tag{3.32}$$

and correspondingly, the inner product $\underline{\gamma}_m^T \underline{\gamma}_m$ is given by

$$B_m^2 = \underline{\gamma}_m^T(t)\underline{\gamma}_m(t) = B^2 - 2C^2 + C^2 = B^2 - C^2 \tag{3.33}$$

For the minimum norm solution

$$B_m^2 = B_m^2 - C_m^2$$

or

$$C_m = \underline{\beta}^T \underline{\gamma}_m = 0 \tag{3.34}$$

The algorithm of Junkins and Turner [10] can be simplified if the constraint equation (3.34) is used instead of rigorous minimization of $\underline{\gamma}^T \underline{\gamma}$.

Since the four Euler parameters are constrained by Eq. (3.4), it is proposed to impose terminal conditions on three of them only; leaving one of the terminal condition unspecified, provides a check on the numerical results. Note that Eq. (3.4) is a rigorous exact integral of the kinematical equation (3.5) for arbitrary $\underline{\omega}(t)$.

3.5 NUMERICAL EXAMPLE

Example 3.1

An optimal detumble and reorientation maneuver is considered here. The spacecraft moments of inertia are the same as those in Example 2.2. The boundary conditions are given in Table 3.1.

The initial conditions correspond to an arbitrarily tumbling spacecraft, with an instantaneous attitude such that the direction cosines of the principal line $\hat{\ell}_{nb}$ are $(1/\sqrt{3}, 1/\sqrt{3}, 1/\sqrt{3})$ and the principal angle ϕ_{nb} is 100°. The final conditions require nulling of

the spacecraft angular rates and reorientation such that the body axes coincide with the inertial frame. The maneuver time is 100 sec. The problem was solved by the Chebyshev method, as well as the method of particular solutions.

Ten basis functions were used for the Chebyshev (collocation) method with uniform sampling. The number of basis functions is enough to represent the integrated solution obtained by the method of particular solutions up to three or four figures. Though the method of collocation requires the orthogonality constraint (or any such constraint given by Eq. (3.18)) to converge to a solution, the method of particular solutions does not need such a constraint unless one wants the minimum norm or some other constrained solution. The missing initial conditions obtained from the two methods are given in Table 3.2.

Figures 3.2, 3.3, and 3.4 show the optimal trajectories of the states $\underline{\beta}$ and $\underline{\omega}$, and the optimal controls respectively. Comparing the $\underline{\omega}$ histories for Examples 3.1 and 2.2, one notices that even though the angular velocity boundary conditions and the maneuver time are the same for both the maneuvers, the inclusion of attitude boundary conditions has considerably altered the control histories and hence the $\underline{\omega}$ histories.

3.6 CONCLUDING REMARKS

The developments in this chapter are motivated by the work of Junkins and Turner [10]. The analytical results presented are purely kinematic and they hold for optimal maneuvers in which a motion with respect to a reference frame is described by Euler parameters. They are

valid for all forms of Euler's equations, i.e., for the cases of flexible vehicles and multiple rigid bodies etc., and all choices of performance indices, as long as β_i do not appear in them either explicitly or implicitly.

TABLE 3.1

Boundary Conditions for Example 3.1

State	Initial Condition (t = 0)	Final Condition (t = T = 100 sec.)
β_0	.64278761	1
β_1	.44227597	0
β_2	.44227597	0
β_3	.44227597	0
ω_1	.01 r/s	0
ω_2	.005 r/s	0
ω_3	.001 r/s	0

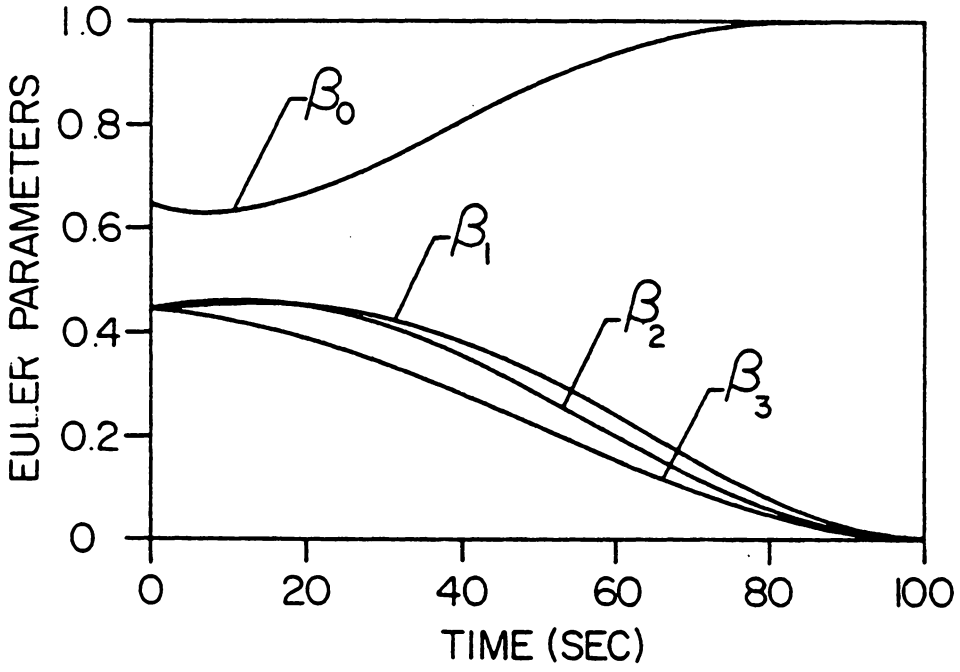

Fig. 3.2 Euler parameters for Example 3.1.

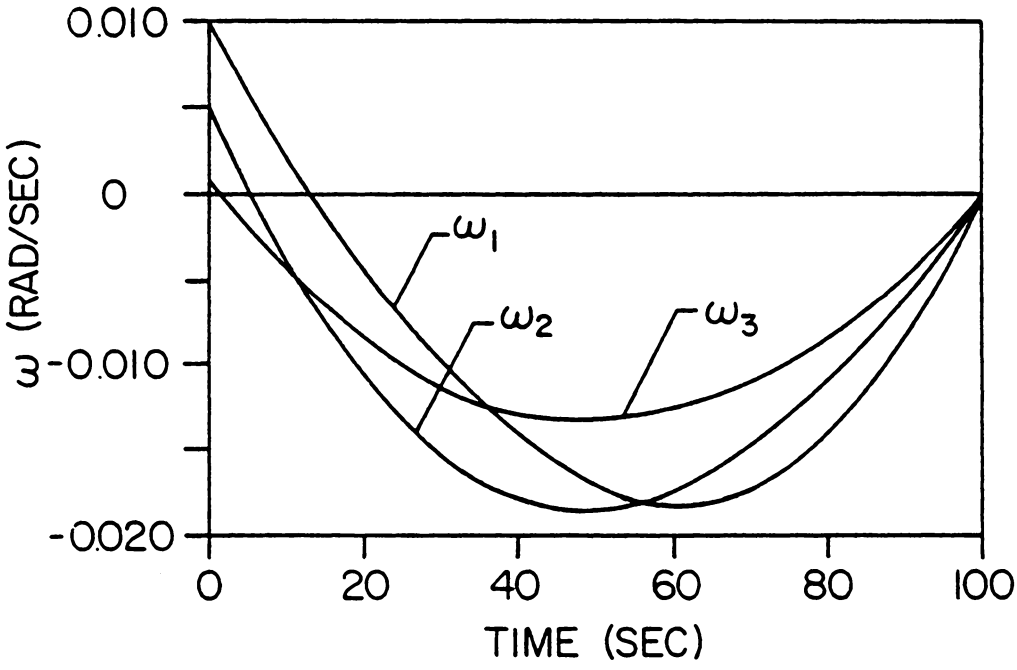

Fig. 3.3 Angular velocity components for Example 3.1.

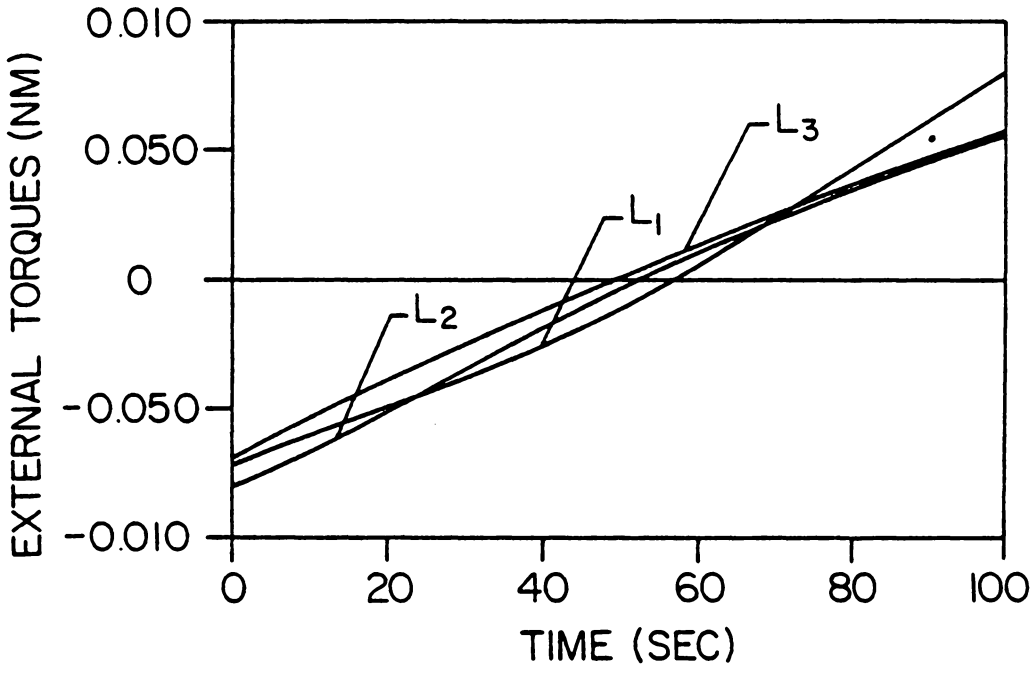

Fig. 3.4 Optimal external torque histories for Example 3.1.

TABLE 3.2

Results of Example 3.1

Missing Initial Condition	Collocation Uniform Sampling NB = 10 Minimum Norm Solution	Method of Particular Solutions
γ_0	-.3396	-.6534
γ_1	.1871	-.2888
γ_2	.0899	-.1259
γ_3	.2164	0
λ_1	6.2441	6.2468
λ_2	6.9153	6.9108
λ_3	7.8690	7.8603

CHAPTER IV

SPACECRAFT ATTITUDE MANEUVERS WITH REACTION WHEELS

Two commonly used momentum exchange devices for spacecraft attitude control are reaction wheels and control moment gyros (CMGs). Reaction wheels retain fixed orientations with respect to the spacecraft and control is imparted by a change in the speed of rotation. CMGs on the other hand usually have fixed-speed rotors but can be gimbaled with respect to the spacecraft. Reaction wheels are suitable for low to medium authority controls desirable for fragile spacecraft. CMGs can provide high authority controls and hence have rapid slew capabilities. Moreover their fixed-speed excites a limited number of modes of flexural vibrations, however there exist analytical difficulties and controllability problems due to the singular states of the gimbal axes for which no control can be imparted to the spacecraft [34]. In this dissertation we are interested primarily in the reaction wheel configurations for attitude control.

It has been established that a spacecraft initially spinning about its axis of maximum moment of inertia, equipped with a reaction wheel mounted on either the axis of least or intermediate inertia can be maneuvered close to a three axis mode by torquing the wheel, such that a specified relative spin rate is maintained between the spacecraft and the wheel. Barba and Aubrun [6] presented a mathematical description of the problem and gave a geometrical interpretation of the energy and momentum transfer through the intersections of the 'momentum sphere' and the 'energy ellipsoid'. Gebman and Mingori [5] made an elegant

perturbation analysis of a similar problem by the multiple scales approach to matched asymptotic expansions. Junkins [7] presented a multiple reaction wheel formulation with Euler parameter kinematics for large angle maneuvers of asymmetric spacecraft.

In this chapter the optimal control problem for an asymmetric spacecraft with three reaction wheels is formulated [35]. Different integral performance criteria are selected based on the control torques, derivatives thereof, and the power required. For an alternate formuation based on a performance index involving the electrical power and an inequality torque constraint, see [13,14].

4.1 SPACECRAFT AND REACTION WHEEL DYNAMICS

A rigid asymmetric spacecraft with three identical reaction wheels (configured to lie along each of the principal axes of inertia) is shown in Fig. 4.1.

The angular momentum of the system (spacecraft and wheels), $\underline{H}$ is given as

$$\underline{H} = \underline{H}_{\text{spacecraft}} + \underline{H}_{\text{wheels}}. \tag{4.1}$$

In terms of the various angular velocities (ω_1, ω_2 and ω_3 of the spacecraft and Ω_1,Ω_2 and Ω_3 of the wheels) and the principal moments of inertia (I_1^*,I_2^* and I_3^* of the spacecraft, $J_{a(\text{axial})}$ and $J_{t(\text{transverse})}$ of the wheels) the angular momentum vector in the body frame can be written as

$$\begin{aligned}\underline{H} = {} & I_1\omega_1\hat{\underline{b}}_1 + I_2\omega_2\hat{\underline{b}}_2 + I_3\omega_3\hat{\underline{b}}_3 \\ & + h_1\hat{\underline{b}}_1 + h_2\hat{\underline{b}}_2 + h_3\hat{\underline{b}}_3\end{aligned} \tag{4.2}$$

where

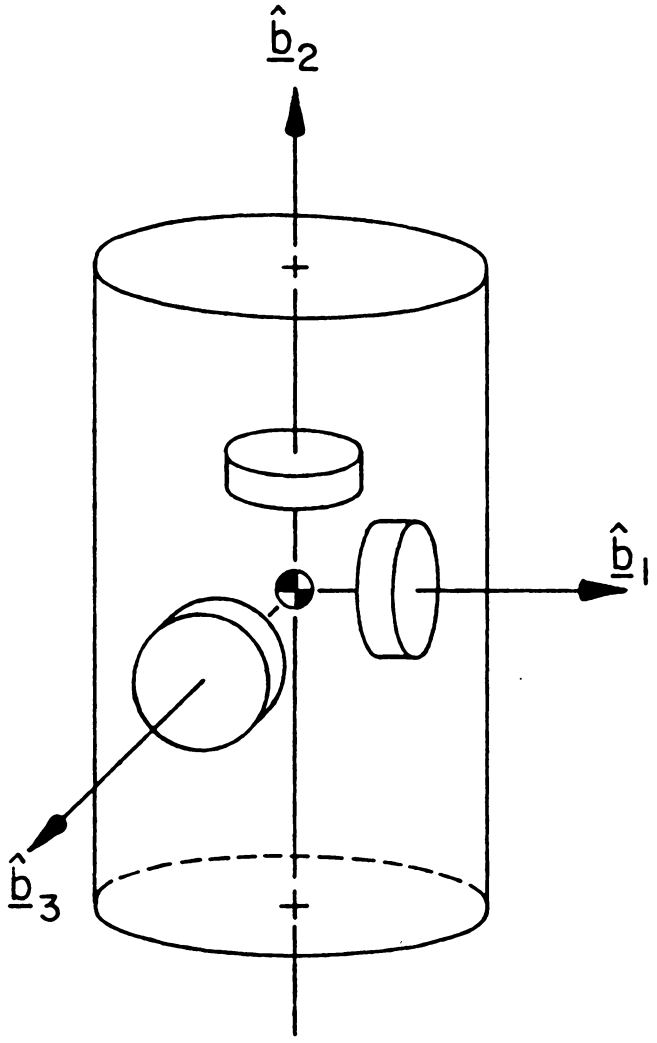

Fig. 4.1 Rigid spacecraft with three orthogonal reaction wheels.

$$\left.\begin{aligned} I_i &= I_i^* + J_a + 2J_t \\ h_i &= J_a \Omega_i, \text{ wheel relative angular momentum} \end{aligned}\right\} i=1,2,3.$$

In the absence of external torques the angular momentum vector is conserved in inertial space. Hence

$$\frac{d}{dt}(\underline{H})_n = \frac{d}{dt}(\underline{H})_b + \underline{\omega} \times \underline{H} = 0 \tag{4.3}$$

For the i^{th} wheel, the motor torque u_i is given by the following equation:

$u_i = \frac{d}{dt}$ [axial component of the angular momentum of the i^{th} wheel],

or

$$u_i = \frac{d}{dt}[J_a(\omega_i + \Omega_i)] = J_a\dot{\omega}_i + \dot{h}_i. \tag{4.4}$$

The equations of the spacecraft and wheel angular motions are finally obtained by using eqs. (4.3) and (4.4) as

$$\begin{aligned} (I_1 - J_a)\dot{\omega}_1 &= (I_2 - I_3)\omega_2\omega_3 - h_3\omega_2 + h_2\omega_3 - u_1 \\ (I_2 - J_a)\dot{\omega}_2 &= (I_3 - I_1)\omega_3\omega_1 - h_1\omega_3 + h_3\omega_1 - u_2 \\ (I_3 - J_a)\dot{\omega}_3 &= (I_1 - I_2)\omega_1\omega_2 - h_2\omega_1 + h_1\omega_2 - u_3 \end{aligned} \tag{4.5}$$

and

$$\dot{h}_i = u_i - J_a\dot{\omega}_i \ , \quad i = 1,2,3.$$

4.2 MOTION RELATIVE TO THE ANGULAR MOMENTUM FRAME

The inertial frame $\{\hat{\underline{n}}\}$ implicit in the above discussion is quite arbitrary. Since only internal torques are admitted, we know that the system angular momentum is constant.

Significant advantages are realized by introducing a special inertial frame $\{\hat{h}\}$ such that $\underline{H} = H\,\hat{h}_2$ as shown in Fig. 4.2. We will see below that making use of the "angular momentum integral" in this fashion effectively reduces the order of the system of equations (4.5). The directions of the other two unit vectors are arbitrary except for a rotation about $\hat{h}_2$; these two directions can be specified by any convenient rule such as the one given by Kraige and Junkins [36], which we use.

The orientation of body-fixed principal axes $\{\hat{b}\}$ with respect to the $\{\hat{h}\}$ frame is given by

$$\{\hat{b}\} = [C(\underline{\delta})]\{\hat{h}\}, \tag{4.6}$$

where $\delta_0, \delta_1, \delta_2, \delta_3$ are a new set of time varying Euler parameters. The orientation of the $\{\hat{n}\}$ frame with respect to the $\{\hat{h}\}$ frame is given by

$$\{\hat{n}\} = [C(\alpha)]\{\hat{h}\}, \tag{4.7}$$

where $\alpha_0, \alpha_1, \alpha_2, \alpha_3$ are constant Euler parameters, since both $\{\hat{n}\}$ and $\{\hat{h}\}$ are inertial frames. These Euler parameters are related to the corresponding principal direction cosines and the principal angle as

$$\begin{aligned} \alpha_0 &= \cos\,(\phi_{hn}/2), \\ \alpha_i &= \ell_{hni}\,\sin\,(\phi_{hn}/2) \quad , \quad i = 1,2,3 \end{aligned} \tag{4.8}$$

The angle ϕ_{hn}, between $\underline{H}$ and $\hat{n}_2$ is defined as

$$\phi_{hn} = \cos^{-1}\,(H_{n2}/H) \quad , \quad 0 < \phi_{hn} < \pi, \tag{4.9}$$

where $\underline{H} = H_{n1}\hat{n}_1 + H_{n2}\hat{n}_2 + H_{n3}\hat{n}_3 = H_{b1}\hat{b}_1 + H_{b2}\hat{b}_2 + H_{b3}\hat{b}_3 = H_{h1}\hat{h}_1 + H_{h2}\hat{h}_2 + H_{h3}\hat{h}_3$. The axis of rotation $\hat{I}_{hn}$ is a unit vector normal to the plane of $\underline{H}$ and $\hat{n}_2$:

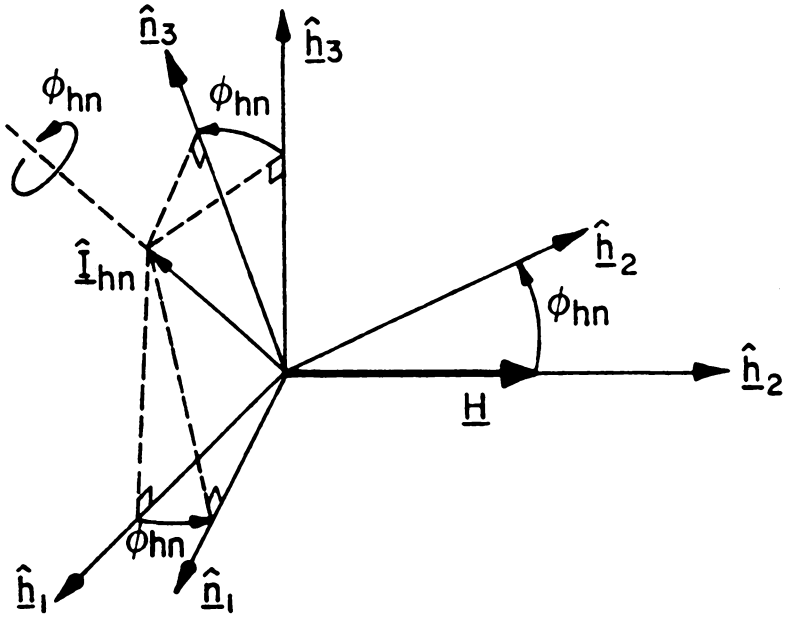

Fig. 4.2 Principal rotation ϕ_{hn} about $\hat{I}_{hn}$ defining the orientation of $\{\hat{n}\}$ with respect to $\{\hat{h}\}$.

$$\hat{\underline{I}}_{hn} = \frac{\underline{H} \times \hat{\underline{n}}_2}{|\underline{H} \times \hat{\underline{n}}_2|} = (H_{n1}^2 + H_{n2}^2)^{-1/2} (H_{n1}\hat{\underline{n}}_3 - H_{n3}\hat{\underline{n}}_1) \tag{4.10}$$

We note that if $\underline{H}$ is parallel to $\hat{\underline{n}}_2$ we can reorient the $\{\hat{\underline{h}}\}$ frame such that $\underline{H}$ is parallel to either $\hat{\underline{h}}_1$ or $\hat{\underline{h}}_3$.

Using eqs. (4.8), (4.9) and (4.10) we obtain expressions for the Euler parameters $\{\alpha\}$:

$$\begin{aligned}
\alpha_0 &= (H + H_{n2})^{1/2}/(2H)^{1/2}, \\
\alpha_1 &= -H_{n3}(H - H_{n2})^{1/2}/[2H(H_{n1}^2 + H_{n3}^2)]^{1/2}, \\
\alpha_2 &= 0, \\
\alpha_3 &= H_{n1}(H - H_{n2})^{1/2}/[2H(H_{n1}^2 + H_{n3}^2)]^{1/2}.
\end{aligned} \tag{4.11}$$

It can be shown that

$$[C(\delta)] = [C(\beta)][C(\alpha)] \tag{4.12}$$

The Euler parameters $\delta_i(t)$ can be obtained in terms of $\beta_i(t)$ and α_i by the following analogous successive rotation result due to Whittaker [32]:

$$\begin{Bmatrix} \delta_0 \\ \delta_1 \\ \delta_2 \\ \delta_3 \end{Bmatrix} = \begin{bmatrix} \beta_0 & -\beta_1 & -\beta_2 & -\beta_3 \\ \beta_1 & \beta_0 & \beta_3 & -\beta_2 \\ \beta_2 & -\beta_3 & \beta_0 & \beta_1 \\ \beta_3 & \beta_2 & -\beta_1 & \beta_0 \end{bmatrix} \begin{Bmatrix} \alpha_0 \\ \alpha_1 \\ \alpha_2 \\ \alpha_3 \end{Bmatrix} \tag{4.13}$$

The angular momentum vector can now be expressed in the body frame:

$$\begin{Bmatrix} H_{b1} \\ H_{b2} \\ H_{b3} \end{Bmatrix} = [C(\delta)] \begin{Bmatrix} 0 \\ H \\ 0 \end{Bmatrix} = \begin{Bmatrix} 2(\delta_1\delta_2 + \delta_0\delta_3)H \\ (\delta_0^2 - \delta_1^2 + \delta_2^2 - \delta_3^2)H \\ 2(\delta_2\delta_3 - \delta_0\delta_1)H \end{Bmatrix} \tag{4.14}$$

Hence, the wheel angular velocities may be expressed as

$$h_i = J_a\Omega_i = H_{bi}(\delta) - I_i\omega_i \ , \ i = 1,2,3. \tag{4.15}$$

Eliminating h_i from eq. (4.5) we obtain

$$(I_1 - J_a)\dot{\omega}_1 = - H_{b3}(\delta)\omega_2 + H_{b2}(\delta)\omega_3 - u_1$$
$$(I_2 - J_a)\dot{\omega}_2 = - H_{b1}(\delta)\omega_3 + H_{b3}(\delta)\omega_1 - u_2 \qquad (4.16)$$
$$(I_3 - J_a)\dot{\omega}_3 = - H_{b2}(\delta)\omega_1 + H_{b1}(\delta)\omega_2 - u_3$$

Equations (3.5) in terms of δ_i are given by

$$\underline{\dot{\delta}} = [G(\omega)]\underline{\delta} \qquad (4.17)$$

Equations (4.16) and (4.17) are now used to model the system dynamics and orientation respectively. The seven states are the elements of $\{\underline{\delta}\}$ and $\{\underline{\omega}\}$.

4.3 THE OPTIMAL CONTROL PROBLEM

We now state the optimal control problem: Given the states at the initial and final times, determine the control torque histories that will transfer the system from the initial to the final state in a prescribed time, T, while minimizing a suitable performance index.

In this regard we seek maneuvers which minimize one of the three performance indices based on control torques and their time derivatives:

$$J_{k+1} = \frac{1}{2}\int_0^T \left[\sum_{i=1}^{3} (d^k u_i(t)/dt^k)^2\right]dt, \qquad (4.18)$$

$k = 0,1,2.$

The indices of eq. (4.18) emphasize smallness of the control magnitude and (in the k = 1,2 case) smoothness of the control and control rate. In addition, for each optimal maneuver, we obtain a positive measure of electrical energy expenditure, by computing the following integral (E):

$$E = \int_o^T \sum_{i=1}^{3} |u_i(t)\Omega_i(t)|dt \qquad (4.19)$$

as a "side calculation".

4.4 NECESSARY CONDITIONS FOR OPTIMALITY

Necessary Conditions with J_1:

The Hamiltonian F for the system of equations (4.16) and (4.17), and performance index J_1, is defined as

$$F \equiv \frac{1}{2} \sum_{i=1}^{3} u_i^2 + \sum_{i=0}^{3} \gamma_i \dot{\delta}_i + \sum_{i=1}^{3} \lambda_i \dot{\omega}_i \tag{4.20}$$

where γ_i and λ_i are Lagrange multipliers, or co-states. The state and co-state equations are obtained by the application of Pontryagin's principle (Appendix A). The state equations are as follows:

$$\begin{aligned}
\dot{\underline{\delta}} &= [k(\delta)] \begin{Bmatrix} 0 \\ \underline{\omega} \end{Bmatrix} \\
\dot{\omega}_1 &= (-H_{b3}(\delta)\omega_2 + H_{b2}(\delta)\omega_3)/(I_1 - J_a) - \lambda_1/(I_1 - J_a)^2 \\
\dot{\omega}_2 &= (-H_{b1}(\delta)\omega_3 + H_{b3}(\delta)\omega_1)/(I_2 - J_a) - \lambda_2/(I_2 - J_a)^2 \\
\dot{\omega}_3 &= (-H_{b2}(\delta)\omega_1 + H_{b1}(\delta)\omega_2)/(I_3 - J_a) - \lambda_3/(I_3 - J_a)^2
\end{aligned} \tag{4.21}$$

The co-state equations follow directly from the partial derivatives

$$\dot{\gamma}_i = -\frac{\partial F}{\partial \delta_i} \quad , \quad \dot{\lambda}_j = -\frac{\partial F}{\partial \omega_j}, \tag{4.22}$$

for i = 0,1,2,3 and j = 1,2,3, upon replacing $\dot{\delta}_i$ and $\dot{\omega}_j$ in eq. (4.20) by eqs. (4.16) and (4.17).

Necessary Conditions with J_2:

The necessary conditions for optimal maneuvers subject to the performance index J_2, are obtained in a fashion similar to that

described above, with the exception that the torques (u_i) are treated as states instead of controls as shown.

We define three new pseudo states (u_i) given by the following differential equations

$$\frac{d}{dt}(u_i) = \dot{u}_i = \bar{u}_i, \tag{4.23}$$

where $\bar{u}_i$, i = 1,2,3 are the controls. Next the new Hamiltonian F is written as

$$F = \frac{1}{2}\sum_{i=1}^{3}\bar{u}_i^2 + \sum_{i=0}^{3}\gamma_i\dot{\delta}_i + \sum_{i=1}^{3}\lambda_i\dot{\omega}_i + \sum_{i=1}^{3}c_i\dot{u}_i \tag{4.24}$$

where c_i are additional co-states.

The extremality of F leads to the following choice for $\bar{u}_i$:

$$\frac{\partial F}{\partial \bar{u}_i} = 0 = \bar{u}_i + c_i \rightarrow \bar{u}_i = -c_i \tag{4.25}$$

The state equations are given by (4.16) and (4.17). The co-state equations can be derived using Eq. (4.24) in Eqs. (4.22), and using $\dot{c}_i = -\frac{\partial F}{\partial \bar{u}_i} = \lambda_i/(I_i - J_a)$. Upon eliminating c_i and $\bar{u}_i$, using Eqs. (4.23) and (4.25), this leads to an optimal control satisfying the differential equation

$$\ddot{u}_i = -\lambda_i/(I_i - J_a) \tag{4.26}$$

Two arbitrary boundary conditions can now be prescribed on u_i (i.e., $u_i(0)$ and $u_i(T)$) as if they were states.

Necessary Conditions With J_3

The state, co-state equations can be derived in a manner described above. We find the optimal control satisfies the 4^{th} order differential equation

$$d^4u_i/dt^4 = \lambda_i/(I_i - J_a) \tag{4.27}$$

We are now in a position to prescribe four boundary conditions on u_i and $\dot{u}_i$. This is a form of torque shaping, permitting zero control and control rates initially and finally; such maneuvers are smooth and would excite high frequency flexural modes of the spacecraft to a lesser degree when compared to the two previous maneuvers.

4.5 BOUNDARY CONDITIONS AND THE TWO-POINT BOUNDARY VALUE PROBLEM

For a completely controllable spacecraft configuration (Fig. 4.1), given the initial conditions, the final angular velocity and orientation states are arbitrary as long as the system angular momentum is conserved, as given by eq. (4.14). Hence the initial and final states are known but the initial co-states are unknown; the state, co-state differential equations with such split boundary conditions form a two-point boundary value problems (TPBVP).

Another class of TPBVP's arises for special optimal maneuvers of spacecraft which are not completely controllable (in the above sense), due to their reaction wheel configurations (Fig. 4.3); such an optimal maneuver is considered in Example 4.1. For arbitrary initial state, one can only desire a final state but cannot exactly achieve it in finite time. Hence these maneuvers are optimal in the sense that they transform the system from the given intial conditions to a final state

which is as close as possible to the desired final state. The performance index in such cases includes the control torques and the errors in the final states (the differences between the achieved and the desired final states) as well. Interestingly, application of the Pontryagin's principle then provides terminal conditions on the co-states in terms of the error (sometimes the errors are weighted by a weighting factor) in the desired final states.

Single axis analytical solutions can be obtained in a manner very similar to those obtained for external torque maneuvers, by Junkins and Turner [10].

4.6 ILLUSTRATIVE EXAMPLES

Maneuvers of interest are considered for two spacecraft configurations. The method of particular solutions is used for computation of optimal controls.

Example 4.1: The One Wheel Maneuver.

We consider here an optimal detumble and reorientation maneuver similar to the flat-spin recovery of a dual-spin spacecraft. It is desired to reorient the spin stablized spacecraft (spinning initially about $\underline{\hat{b}}_3$, wheel along $\underline{\hat{b}}_2$ and initially locked relative to spacecraft) and simultaneously bring it to a three-axis controlled mode (Fig. 4.3) by torquing the wheel in an optimal fashion. Without considering the evolution of the attitude, we look at the momentum dynamics. Equations (4.5), for the present example reduce to

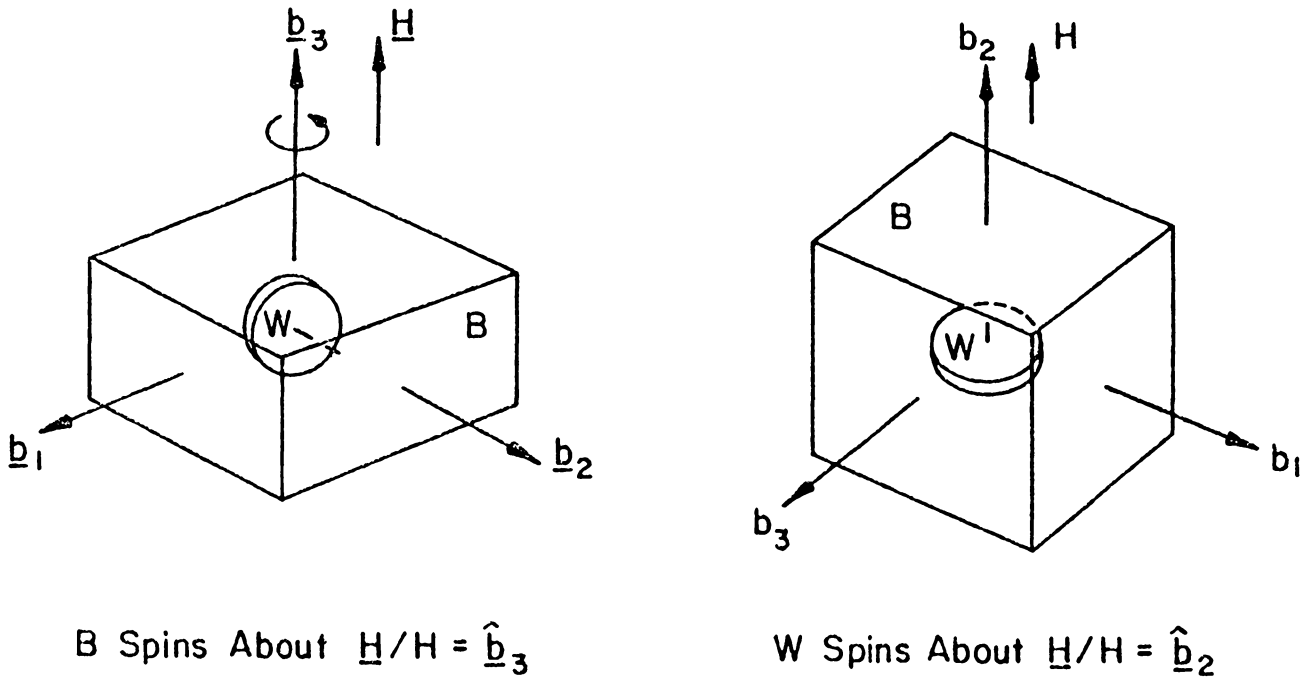

Fig. 4.3 Given initial state and desired final state for the spacecraft of Example 4.1.

$$
\begin{aligned}
I_1\dot{\omega}_1 &= (I_2 - I_3)\omega_3\omega_2 + h\omega_3 \\
I_2^*\dot{\omega}_2 &= (I_3 - I_1)\omega_1\omega_3 - u \\
I_3\dot{\omega}_3 &= (I_1 - I_2)\omega_1\omega_2 - h\omega_1 \\
\dot{h} &= u - J_a\dot{\omega}_2
\end{aligned}
\tag{4.28}
$$

where

$$I_1 = I_1^* + J_t,\ I_2 = I_2^* + J_a,\ I_3 = I_3^* + J_t$$

The spacecraft parameters and the boundary conditions are given in Table 4.1.

Ideally at the final time, $\underline{\hat{b}}_2$ should be parallel to $\underline{H}$, but inspection of the dynamic equations (4.28) reveals that it is impossible to exactly obtain the desired final state (null terminal angular rates in a finite time) from the initial state with continuous torques; due to the so called uncontrollable configuration. A residual nutation is unavoidable without the use of energy dissipation mechanisms (e.g., nutation dampers). The nutation angle θ is defined as the angle between $\underline{H}$ and $\underline{\hat{b}}_2$:

$$\theta = \cos^{-1}(H_{b2}/H) = \cos^{-1}[(I_2\omega_2 + h)/H] \tag{4.29}$$

An excellent nominal maneuver strategy is to torque the wheel such that the time derivative of the wheel relative angular momentum (h) is kept constant, Fig. (4.4). It is noted that the torque history for such a maneuver is <u>not constant</u>. As discussed above, we use the following performance index:

$$J_4 = \frac{1}{2}\left[\sum_{i=1}^{3}\omega_i^2(T)\right] + \frac{1}{2}\int_0^T u^2 dt \tag{4.30}$$

The Hamiltonian F is defined as

Table 4.1

Spacecraft Parameters and Boundary Conditions for Example 4.1

Spacecraft Parameters			Boundary Conditions	
Parameter	Value (Kgm^2)	State	Initial Condition (t = 0)	Final Condition (t=T=4000 sec.)
I_1^*	86.215	ω_1	0	0
I_2^*	85.07	ω_2	0	0
I_3^*	113.565	ω_3	.1761 r/s	0
J_a	.05			
J_t	.025	H	0	20.003199 Nms

$$F = \frac{1}{2} u^2 + \sum_{i=1}^{3} \lambda_i \dot{\omega}_i + \alpha \dot{h} \tag{4.31}$$

The optimal control u(t) in terms of the co-states is

$$u(t) = \lambda_2 / I_2^* - \alpha(1 + \frac{J}{I_2^*}) \tag{4.32}$$

Final conditions:

$\lambda_i(T) = \omega_i(T) \quad i = 1,2,3$

$h(T) = H = 20.003199$ Nms.

Starting Solution

A readily usable solution is obtained by setting all the initial co-states to zero except $\alpha(0)$, which is taken as -.005 (this choice is based on eq. (4.32) and the fact that $\dot{h}$ for the nominal maneuver mentioned above, is .005 Nm). On forward integration of state, co-state differential equations we obtain the following terminal states:

$\omega_1(T) = -.0276$ r/s, $\omega_2(T) = .00129$ r/s

$\omega_3(T) = .0093$ r/s, $h(T) = 19.72$ Nms.

Using this nominal solution with algorithm A, we obtained solutions which converged to at least six figures after eight iterations. Using the initial conditions and the converged co-states the nonlinear system of equations when integrated yielded a solution accurate to at least four figures at the final time. Four more iterations with algorithm B resulted in a solution accurate to at least nine figures, at the final time. The converged initial co-states (the figures have been truncated)

are

$\lambda_1(0) = .36690762 \times 10^{-2}$, $\lambda_2(0) = -.92466744 \times 10^{-2}$

$\lambda_3(0) = .81021593 \times 10^{-2}$, $\alpha(0) = -.48258503 \times 10^{-2}$

The final states are

$\omega_1(T) = -.33215662 \times 10^{-2}$, $\omega_2(T) = -.71148036 \times 10^{-3}$,

$\omega_3(T) = -.13458590 \times 10^{-1}$, $h(T) = 20.003199.$

The performance index J_4 and the energy expenditure E (these are easily computed for the constant $\dot{h}$ maneuver) for the two maneuvers are:

Constant $\dot{h}$ maneuver: $J_4 = .050351472 N^2 m^2 s$, E = 3998.23J

Optimal maneuver: $J_4 = .050123966 N^2 m^2 s$, E = 3999.52J.

Compared to the nominal maneuver, the optimal maneuver (Fig. 4.5) is performed with lower amplitude oscillations in ω_1 and ω_3 after 1000 sec., slightly higher oscillations in ω_2 and u before and up to 1000 sec; ω_2 and u are almost linear after this time. The wheel angular momentum (speed) increases but the slope is not constant. Since the wheel moment of inertia is quite small, the oscillations in u are essentially due to oscillations in the slope of h. The pointing error is 7.7° for the constant $\dot{h}$ maneuver; the optimal maneuver reduces the error to 4.2°. It is observed that though the optimal wheel speed history is only slightly varied from that of the nominal maneuver, this difference results in considerable reduction in the pointing error; on the other hand it is easier to implement the former maneuver.

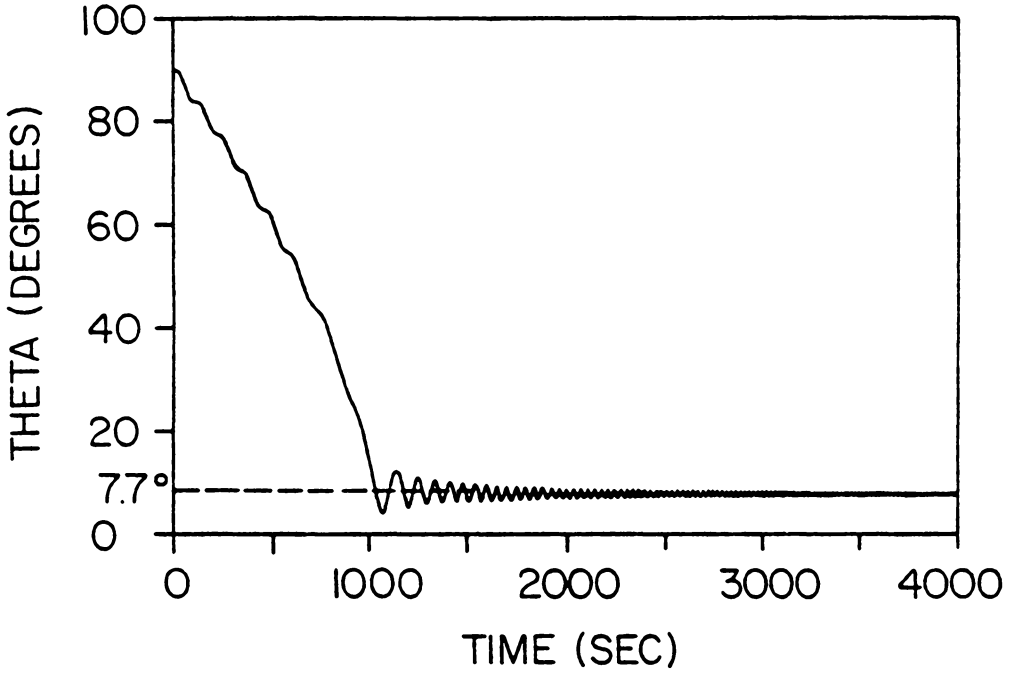

Fig. 4.4 (a) Nutation angle θ for the nominal maneuver.

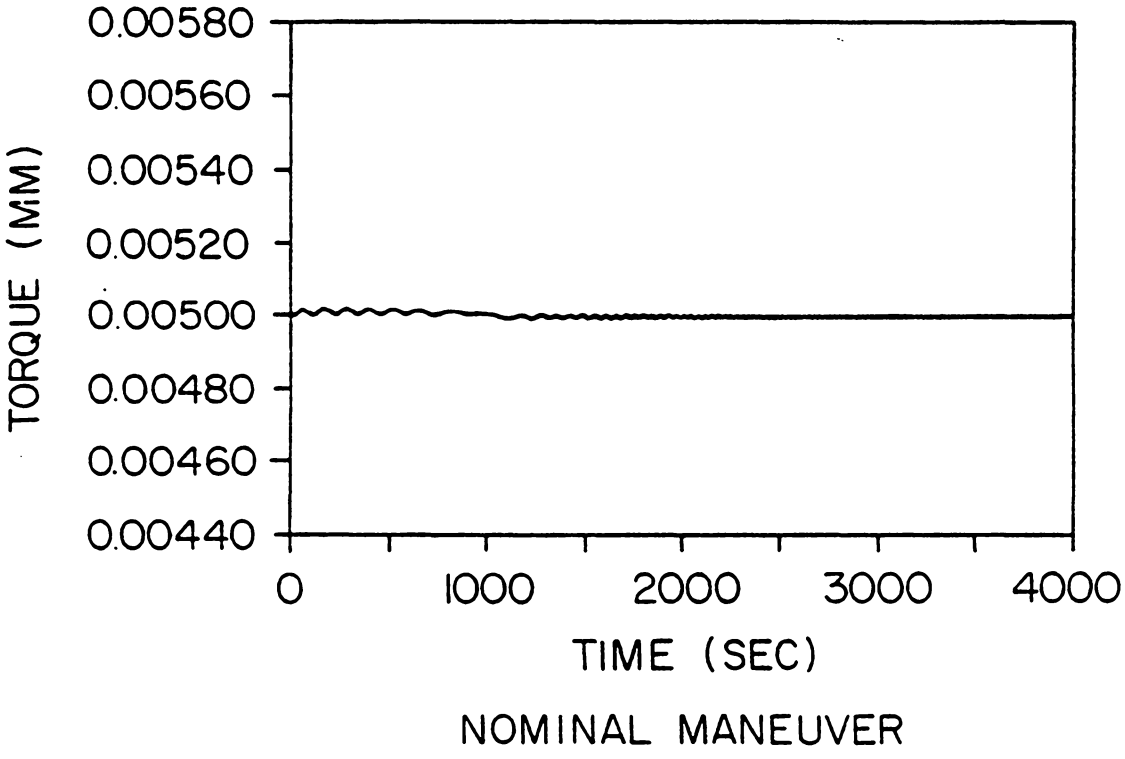

Fig. 4.4 (b) Control torque u for the nominal maneuver.

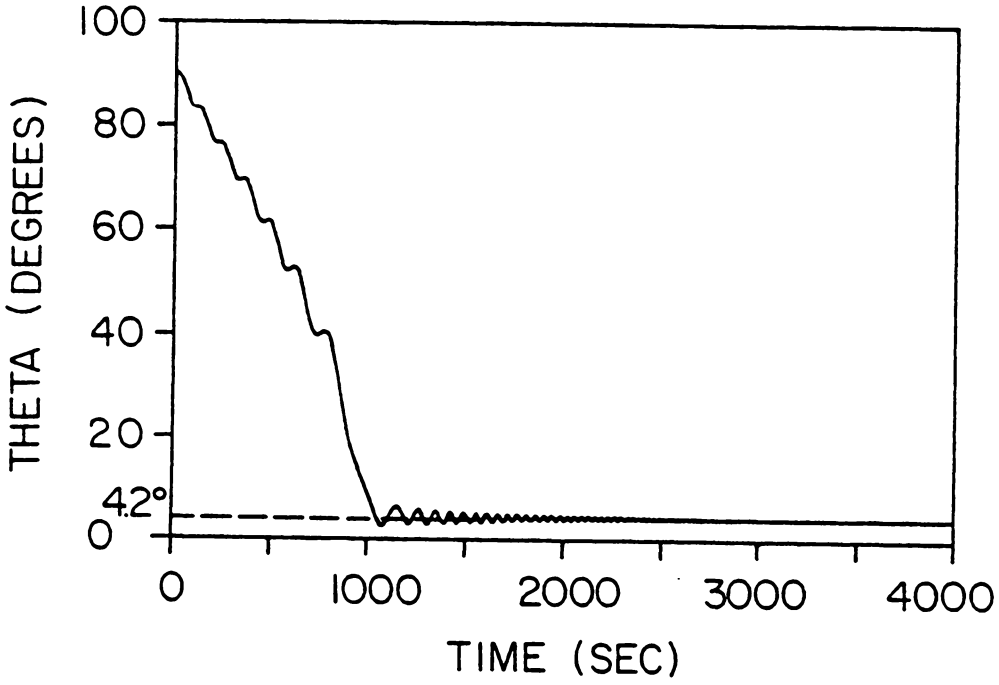

Fig. 4.5 (a) Nutation angle θ for the optimal maneuver.

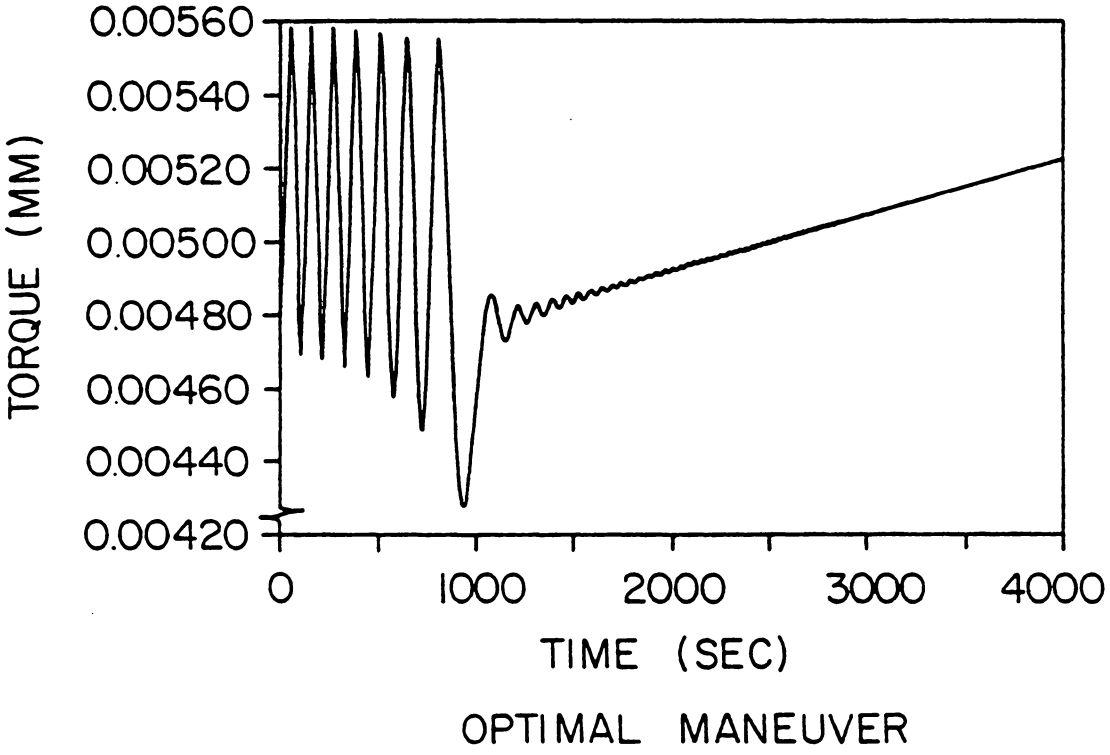

Fig. 4.5 (b) Control torque u for the optimal maneuver.

Example 4.2

A class of more general reorientation and detumble maneuvers can be performed by the three-wheel configuration depicted in Fig. 4.1. We consider one such maneuver and show the effect of different performance indices on the control torque and state histories. The spacecraft parameters (I^*_i and J_a) are the same as before; the boundary conditions are given below in Table 4.2. This maneuver is essentially the same as the one considered in Example 3.1, except for the nature of torque generation. The wheels are initially locked with respect to the spacecraft. The wheel speeds at the final time can be determined in general as:

$$\Omega_i = (H_{bi}(\delta) - I_i\omega_i)/J_a \tag{4.33}$$

The boundary conditions on $\underline{\beta}$ are transformed into boundary conditions on $\underline{\delta}$ by the procedure described previously. As the Euler parameters are constrained by the relation given by eq. (3.4), the boundary condition on $\delta_0(T)$ is not imposed explicitly; leaving δ_0 unconstrained at the final time provides a check on the converged solution.

Starting Solutions

Since the states are known at the initial and final times, a linear interpolation is performed between the two points. All the co-states are assumed to be zero throughout. Method of particular slution (Algorithm A) is used for all computations.

Table 4.2

Boundary Conditions for Example 4.2

State	Initial Conditions (t = 0)	Final Conditions (t = T = 100 sec.)
β_0	.64278761	1
β_1	.44227597	0
β_2	.44227597	0
β_3	.44227597	0
ω_1	.01 r/s	0
ω_2	.005 r/s	0
ω_3	.001 r/s	0
Ω_1	0	H_{n_1}/J_a
Ω_2	0	H_{n_2}/J_a
Ω_3	0	H_{n_3}/J_a

Results

The solutions are accurate up to at least eight significant figures. Figure 4.6, 4.7 and 4.8, show the optimal trajectories and control histories for performance indices J_1, J_2 and J_3 respectively. The number of iterations required and the values of the performance indices are given in Table 4.3. From Fig. 4.6 we see that when J_1 is used as the performance index the torques are non-zero at both the end points. These jump discontinuities in the control would make the spacecraft start and stop with jerks, which is undesirable especially for fragile vehicles. Figures 4.7 and 4.8 show the effects of imposing boundary conditions on the controls and their derivatives respectively. The smooth maneuvers produced by these torques can be seen from the trajectories of the states. Imposing boundary conditions of this nature increases control torque requirements, the angular velocities of the spacecraft and the wheel speeds at intermediate points considerably. The energy requirements increase almost linearly with the constraints imposed on the controls.

A further generalization of the above formulations leads to a performance index of the form

$$J_5 = \frac{1}{2} \int_0^T \sum_{j=1}^{3} [w_{1j} u_j^2 + w_{2j} \dot{u}_j^2 + w_{3j} \ddot{u}_j^2] dt \qquad (4.34)$$

Unless the weights w_{1i} and w_{2i} are small compared to w_{3i}, the TPBVP involves stiff differential equations which we have found to be difficult to solve by Runge-Kutta methods.

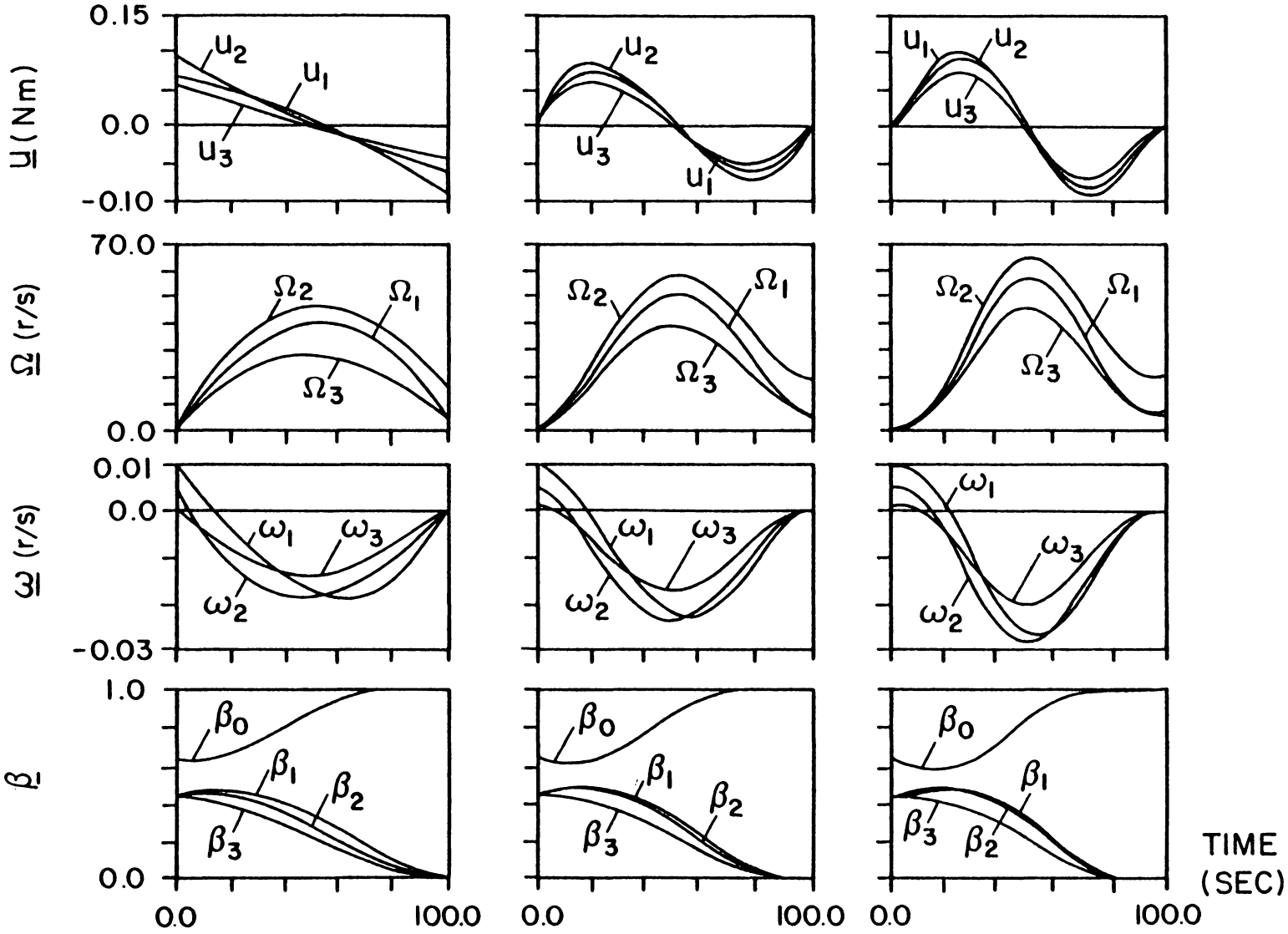

Fig. 4.6 J_1 optimal maneuver

Fig. 4.7 J_2 optimal maneuver

Fig. 4.8 J_3 optimal maneuver

Table 4.3

Results of Example 4.2

Performance Index	No. of Iterations	Performance Index	Energy Index (E) Joules
1	6	.248039	229.457
2	5	.001477	346.501
3	5	.000021	463.682

Example 4.3

In example 4.2 we noticed the increase in the peak wheel speeds and the energy as the control was constrained at the end points. We now consider an alternate performance index which mainly minimizes the control rate, but include a secondary penalty on the electric power. This performance index is

$$J_6 = \frac{1}{2}\int_0^{100} [w \sum_{i=1}^{3} (u_i\Omega_i)^2 + \ddot{\underline{u}}^T\ddot{\underline{u}}]dt \tag{4.35}$$

and the control boundary conditions are

$$u(0) = \dot{u}(0) = u(100) = \dot{u}(100) = 0 \tag{4.36}$$

In attempting to minimize Eq. (4.35) we found the optimal maneuvers were solutions of stiff and extremely sensitive differential equations for w as low as 10^{-6}. This was not surprising and is to be expected if one sees the results of Skaar [13]. The controls associated with minimizing the square of the individual motor powers are characterized by highly nonlinear torque histories which peak sharply initially and finally. After some experimentation, we were able to solve the problem with the following weight function:

$$w = w(t) = 10^{-6}[\tau^4 - 17\tau^3 + \frac{49}{4}\tau^2] \tag{4.37}$$

where

$$\tau = t \qquad t \leq 50$$

$$\tau = 100 - t \qquad t > 50$$

w(t) is a quartic with initial and final magnitudes as well as slopes

equal to zero. The maximum value of w(t) is 10^{-6}. Even though the weight on the power term is quite small, considerable reduction in the maximum wheel speeds and the energy required have been achieved as shown in Table 4.4. The optimal trajectories of $\underline{\omega}$, $\underline{\Omega}$, and the optimal control $\underline{u}$ are shown in Fig. 4.9. Comparison of this maneuver (Fig. 4.9) to the w = 0 optimal maneuver (Fig. 4.8) clearly suggests that a significant tradeoff exists between smoothness of the maneuvers and power consumption/wheel speeds.

4.7 CONCLUDING REMARKS

The optimal large angle attitude maneuver problem has been formulated for an asymmetric spacecraft, with three reaction wheels mounted along its principal axes. The necessary conditions for optimal controls have been derived via the Pontryagin's Principle, for different performance indices. Numerical solutions are presented for example maneuvers. As external torques have been assumed to be negligible at least during the maneuvers, the angular momentum vector is conserved in inertial space. Hence, for given initial spacecraft orientation and body-angular momentum components, one can uniquely determine the final body-angular momentum components, knowing the final attitude; on the other hand knowing the final body-angular momentum components one can specify the spacecraft attitude except for a rotation about the angular momentum vector.

Spacecraft initially tumbling at high angular rates would transfer angular momentum to the wheels if detumbled, making it difficult to maneuver subsequently, unless the wheel momentum is dumped.

Table 4.4

Comparison of Performance Indices J_3 and J_6

Quantity	J_3	J_6
u_{1max} (Nm)	.095	.0965
u_{2max} (Nm)	.1065	.1099
u_{3max} (Nm)	.0767	.0721
Ω_{1mas} (r/s)	56.93	44.38
Ω_{2max} (r/s)	64.37	49.65
Ω_{3max} (r/s)	45.28	35.16
E (J)	463.682	270.004

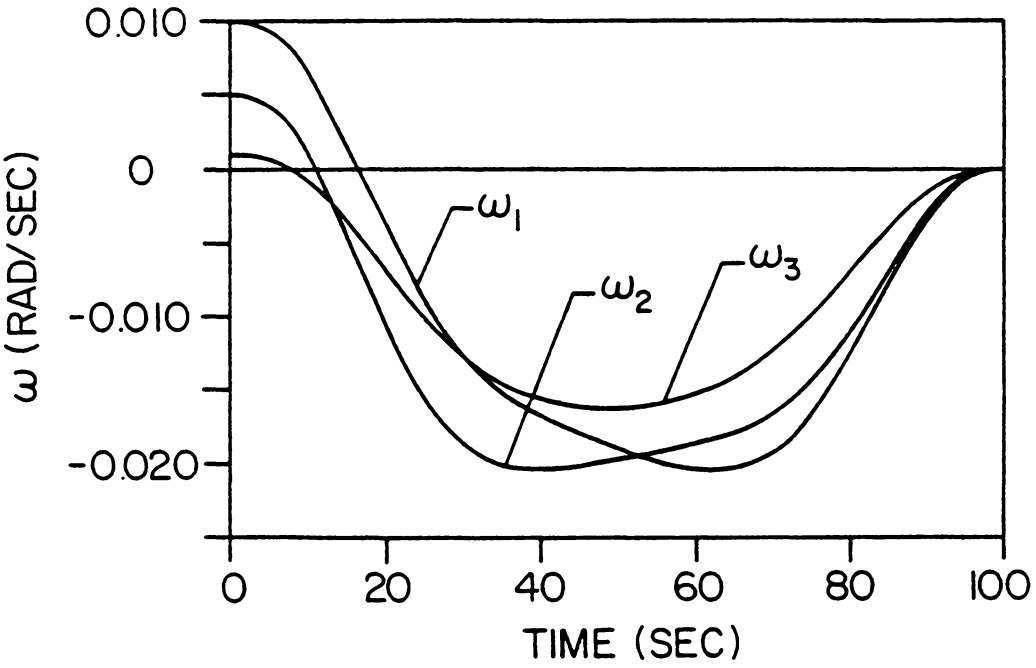

Fig. 4.9 (a) Spacecraft angular velocity components for Example 4.3.

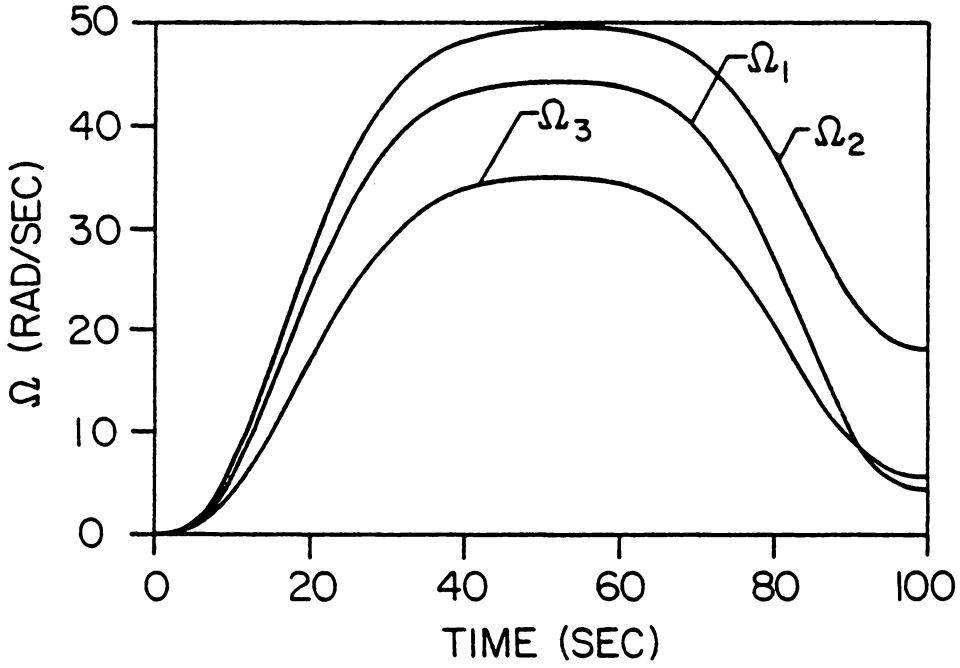

Fig. 4.9 (b) Wheel speeds for Example 4.3.

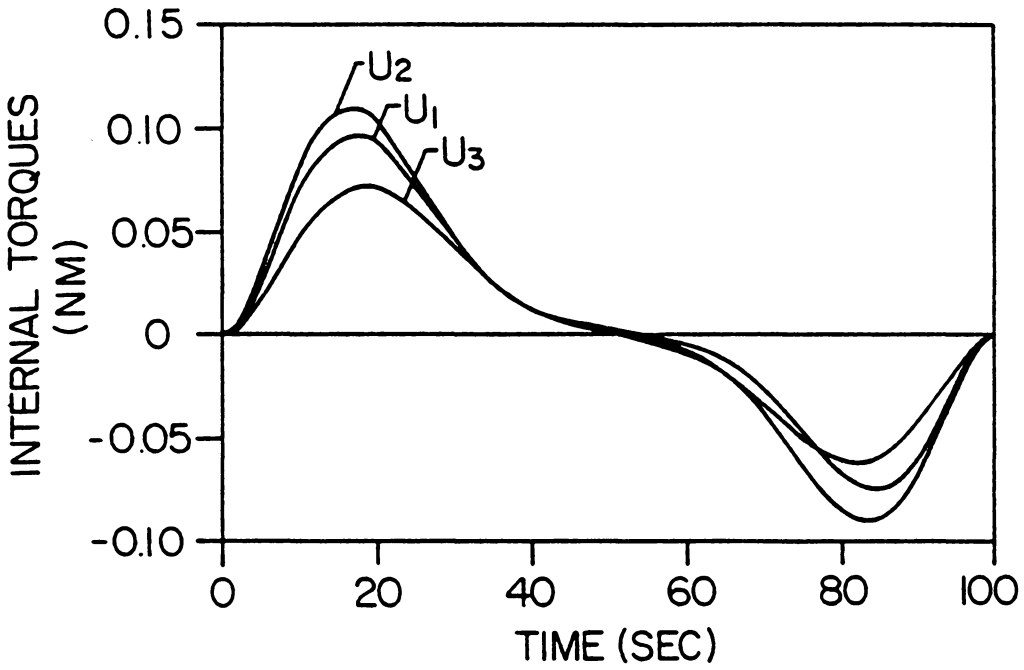

Fig. 4.9 (c) Optimal internal toruqes for Example 4.3.

Simultaneous reorientation, detumbling and wheel momentum dumping can be achieved by maneuvers utilizing both external torques(due to Earth's magnetic field or reaction jets) and momentum transfer. We will present these maneuvers in the next chapter.

CHAPTER V

OPTIMAL ATTITUDE MANEUVERS WITH INTERNAL AND EXTERNAL TORQUES

In Chapter III we delt with optimal spacecraft attitude maneuvers with external torques. If these torques are to be generated by mass expulsion, then tank-stored expendables like hydrazine or cold gas etc. have to be used in large quantities; these systems have limited lifetime and are not suitable for generating precision controls. External torques generated by interaction of onboard electromagnets with the Earth's magnetic field are weak even for low Earth orbits and are not suitable for fast maneuvers; they are functions of spacecraft position and orbital inclination. Solar radiation pressure is of interest at synchronous altitudes but is not practical for optimal attitude control which demands a specific torque history.

In Chapter IV we considered reaction wheel systems for attitude maneuvers and concluded that some form of momentum dumping is necessary without which the control system could be rendered ineffective during the course of the mission. In this chapter a preliminary attempt is made for studying optimal external/internal torque maneuvers. A logical extension is made, of the formulations in Chapters III and IV. It is demonstrated that external torques can be used not only for maneuvering but also for momentum dumping. Though optimal controls are computed, no specific external torque generation scheme is considered, and the issue of whether the commanded external control history can be generated or not is not addressed.

5.1 SPACECRAFT AND REACTION WHEEL DYNAMICS

Following the developments in Chapters III and IV the equations of motion of the spacecraft and reaction wheels can be written down similar to Eqs. (4.5) as the following:

$$(I_1 - J_a)\dot{\omega}_1 = (I_2 - I_3)\omega_2\omega_3 - h_3\omega_2 + h_2\omega_3 - u_1 + L_1$$
$$(I_2 - J_a)\dot{\omega}_2 = (I_3 - I_1)\omega_3\omega_1 - h_1\omega_3 + h_3\omega_1 - u_2 + L_2$$
$$(I_3 - J_a)\dot{\omega}_3 = (I_1 - I_2)\omega_1\omega_2 - h_2\omega_1 + h_1\omega_2 - u_3 + L_3 \qquad (5.1)$$

and

$$\dot{h}_i = u_i - J_a\dot{\omega}_i \quad , \quad i = 1,2,3.$$

The attitude of the spacecraft is given by eqs. (3.7). Hence we have ten state variables $\beta_0,\beta_1,\beta_2,\beta_3,\omega_1,\omega_2,\omega_3,h_1,h_2$, and h_3. As the system angular velocity is not conserved, no further reduction in the dimensionality of the problem can be made.

5.2 OPTIMAL CONTROL

Performance Index:

The performance index selected is an integral over the entire time interval of the maneuver, involving the various torques as follows:

$$J = \frac{1}{2}\int_0^T [w_1(L_1^2 + L_2^2 + L_3^2) + w_2(u_1^2 + u_2^2 + u_3^2)]dt \qquad (5.2)$$

The weights w_1 and w_2 can be adjusted depending on the relative costs and effectiveness of the two modes of torque generation.

Necessary Conditions of Pontryagin:

The Hamintonian (H) of the system of equations (3.7) and (5.1) can be written as

$$H = \frac{1}{2}\{w_1[L_1^2 + L_2^2 + L_3^2] + w_2[u_1^2 + u_2^2 + u_3^2]\}$$

$$+ \underline{\gamma}^T\dot{\underline{\beta}} + \underline{\lambda}^T\dot{\omega} + \underline{\alpha}^T\dot{h}, \qquad (5.3)$$

where $\underline{\alpha}(\alpha_1,\alpha_2,\alpha_3)$ are three additional Lagrange multipliers or co-states corresponding to the three wheel angular momenta h_i. Pontryagin's necessary conditions (Appendix A) lead to the following co-state differential equations

$$\dot{\underline{\gamma}} = -\frac{\partial H}{\partial \underline{\beta}}$$

$$\dot{\underline{\lambda}} = -\frac{\partial H}{\partial \underline{\omega}} \qquad (5.4)$$

$$\dot{\underline{\alpha}} = -\frac{\partial H}{\partial \underline{h}}$$

The optimality conditions are as follows:

$$\frac{\partial H}{\partial L_i} = 0 \quad , \quad i = 1,2,3 \qquad (5.5)$$

$$\frac{\partial H}{\partial u_i} = 0 \quad , \quad i = 1,2,3 \qquad (5.6)$$

Performing differentiations implied in eqs. (5.5) and (5.6) we obtain the following relationships between the controls and the co-states:

$$L_i = (-\lambda_i + J_a\alpha_i)/[w_1(I_i - J_a)] \quad , \quad i = 1,2,3, \qquad (5.7)$$

$$u_i = -\left(\frac{-\lambda_i + I_i\alpha_i}{w_2(I_i - J_a)}\right) \quad , \quad i = 1,2,3. \qquad (5.8)$$

Upon eliminating the controls via eqs. (5.7) and (5.8), in eqs. (5.1) we obtain the state and co-state equations in their final form as follows:

State equations

$$\dot{\underline{\beta}} = [G(\omega)]\underline{\beta}$$

$$\dot{\omega}_1 = \frac{1}{(I_1 - J_a)} [(I_2 - I_3)\omega_2\omega_3 - h_3\omega_2 + h_2\omega_3 + (\frac{-\lambda_1 + I_1\alpha_1}{I_1 - J_a})/w_2 + (\frac{-\lambda_1 + J_a\alpha_1}{I_1 - J_a})/w_1]$$

$$\dot{\omega}_2 = \frac{1}{(I_2 - J_a)} [(I_3 - I_1)\omega_1\omega_3 - h_1\omega_3 + h_3\omega_1 + (\frac{-\lambda_2 + I_2\alpha_2}{I_2 - J_a})/w_2 + (\frac{-\lambda_2 + J_a\alpha_2}{I_2 - J_a})/w_1]$$

$$\dot{\omega}_3 = \frac{1}{(I_3 - J_a)} [(I_1 - I_2)\omega_1\omega_2 - h_2\omega_1 + h_1\omega_2 + (\frac{-\lambda_3 + I_3\alpha_3}{I_3 - J_a})/w_2 + (\frac{-\lambda_3 + J_a\alpha_3}{I_3 - J_a})/w_1] \qquad (5.9)$$

$$\dot{h}_i = \frac{1}{w_2} [\frac{\lambda_i - \alpha_i J_a}{(I_i - J_a)} - \alpha_i] - J_a\dot{\omega}_i \quad , \quad i = 1,2,3 \qquad (5.10)$$

Co-state equations

$$\dot{\underline{\gamma}} = [G(\omega)]\underline{\gamma} \qquad (5.11)$$

$$\dot{\underline{\lambda}}_1 = [\gamma_0\beta_1 - \gamma_1\beta_0 - \gamma_2\beta_3 + \gamma_3\beta_2]/2 + (\frac{-\lambda_2 + \alpha_2 J_a}{I_2 - J_a})[(I_3 - I_1)\omega_3 + h_3] + (\frac{-\lambda_3 + \alpha_3 J_a}{I_3 - J_a})[(I_1 - I_2)\omega_2 - h_2]$$

$$\dot{\lambda}_2 = [\gamma_0\beta_2 + \gamma_1\beta_3 + \gamma_2\beta_0 - \gamma_3\beta_1]/2$$

$$+ \left(\frac{-\lambda_1 + \alpha_1 J_a}{I_1 - J_a}\right)[(I_2 - I_3)\omega_3 - h_3]$$

$$+ \left(\frac{-\lambda_3 + \alpha_3 J_a}{I_3 - J_a}\right)[(I_1 - I_2)\omega_1 + h_1] \qquad (5.12)$$

$$\dot{\lambda}_3 = [\gamma_0\beta_3 - \gamma_1\beta_2 + \gamma_2\beta_1 - \gamma_3\beta_0]/2$$

$$+ \left(\frac{-\lambda_1 + \alpha_1 J_a}{I_1 - J_a}\right)[(I_2 - I_3)\omega_2 + h_2]$$

$$+ \left(\frac{-\lambda_2 + \alpha_2 J_a}{I_2 - J_a}\right)[(I_3 - I_1)\omega_1 - h_1]$$

$$\dot{\alpha}_1 = \frac{-\lambda_3 + J_a\alpha_3}{(I_3 - J_a)}\omega_2 - \frac{-\lambda_2 + J_a\alpha_2}{(I_2 - J_a)}\omega_3$$

$$\dot{\alpha}_2 = \frac{-\lambda_1 + J_a\alpha_1}{(I_1 - J_a)}\omega_3 - \frac{-\lambda_3 + J_a\alpha_3}{(I_3 - J_a)}\omega_1 \qquad (5.13)$$

$$\dot{\alpha}_3 = \frac{-\lambda_2 + J_a\alpha_2}{(I_2 - J_a)}\omega_1 - \frac{-\lambda_1 + J_a\alpha_1}{(I_1 - J_a)}\omega_2$$

Boundary conditions on the states are specified as follows:

$$\beta_i(0) = \beta_{i0} \quad , \quad \beta_i(t) = \beta_{iT} \quad , \quad i = 0,1,2,3 \qquad (5.14)$$

$$\omega_i(0) = \omega_{j0} \quad , \quad \omega_j(T) = \omega_{jT} \quad , \quad j = 1,2,3 \qquad (5.15)$$

$$h_k(0) = h_{k0} \quad , \quad h_k(T) = h_{kT} \quad , \quad k = 1,2,3 \qquad (5.16)$$

5.3 NUMERICAL EXAMPLE

Example 5.1

We consider here the spacecraft of Example 4.2. The initial and final orientation and angular velocities are the same. The initial wheel speeds are zero as before, but the final wheel speeds are also required to be zero. This is a detumbling and reorientation maneuver with simultaneous wheel momentum dumping. We will use the numerical scheme based on the method of particular solutions (Algorithm A). The performance index is

$$J = \frac{1}{2}\int_0^{100} \left[\sum_{i=1}^{3} (L_i^2 + u_i^2)\right]dt \tag{5.17}$$

Fig. 5.1 (a-e) show the optimal trajectories of $\underline{\beta}$, $\underline{\omega}$, $\underline{\Omega}$, and optimal control histories $\underline{L}$, and $\underline{u}$ respectively. Comparing these results with those obtained for Example 4.2, with performance index J_1 we find that there is no appreciable change in $\underline{\beta}$ and $\underline{\omega}$ histories; however there are considerable reductions in the peak Ω_i and peak u_i. Comparing these results with those obtained in Example 3.1, we find a similar trend in $\underline{\beta}$ and $\underline{\omega}$; however the peak L_i are lower.

5.4 CONCLUDING REMARKS

Inclusion of external torques gives added degrees of freedom in the form of three additional boundary conditions on the wheel speeds, which allows arbitrary large angle attitude maneuvers to be performed. The disturbance torques due to gravity gradient and orbital motion have been neglected.

While the present discussion of internal/external torque maneuvers has been restricted to the quadratic index of Eq. (5.2), it is obvious that analogous formulations can be quickly developed to include control derivative penalties or power consumption penalties as in Chapter IV examples.

Excepting the magnetic torques, the other forms of external torques cannot be throttled to generate commanded optimal control histories. Though throttlable reaction jet systems have been designed and used in the Apollo space mission, they are not cost-effective for many present day and planned missions, where very precise control is needed. Moreover the nonuniformity of pairs of parallely operated thrusters would produce forces in addition to torques, causing orbital translations. External, thruster induced torques could be used to maneuver the spacecraft close to the desired state and then internal torques could be used to achieve the precise final orientation. Of course the optimality of this type of hybrid maneuver is a different issue, not treated herein.

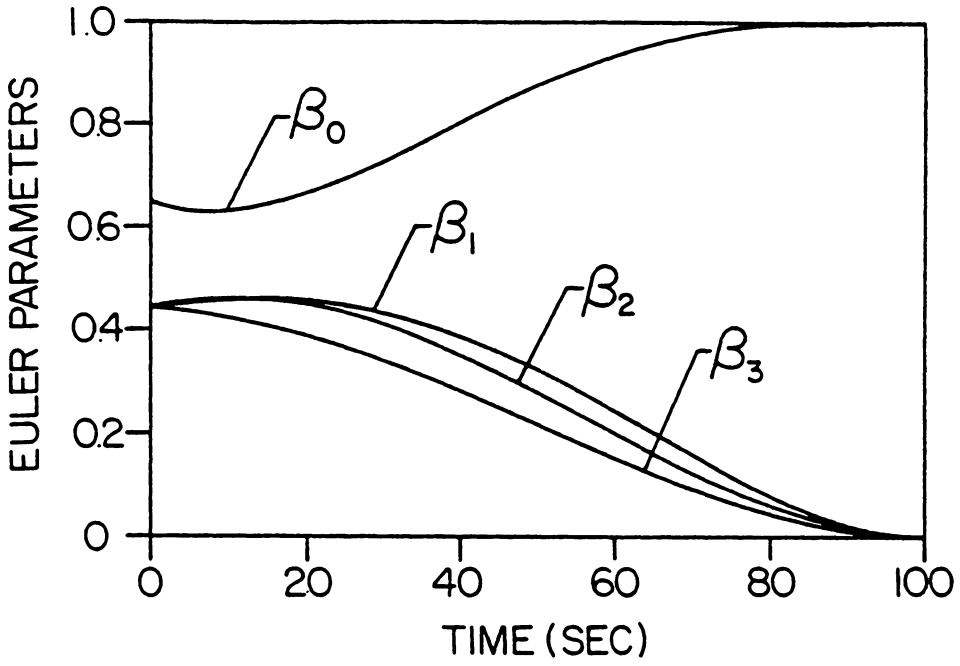

Fig. 5.1 (a) Euler parameters for Example 5.1.

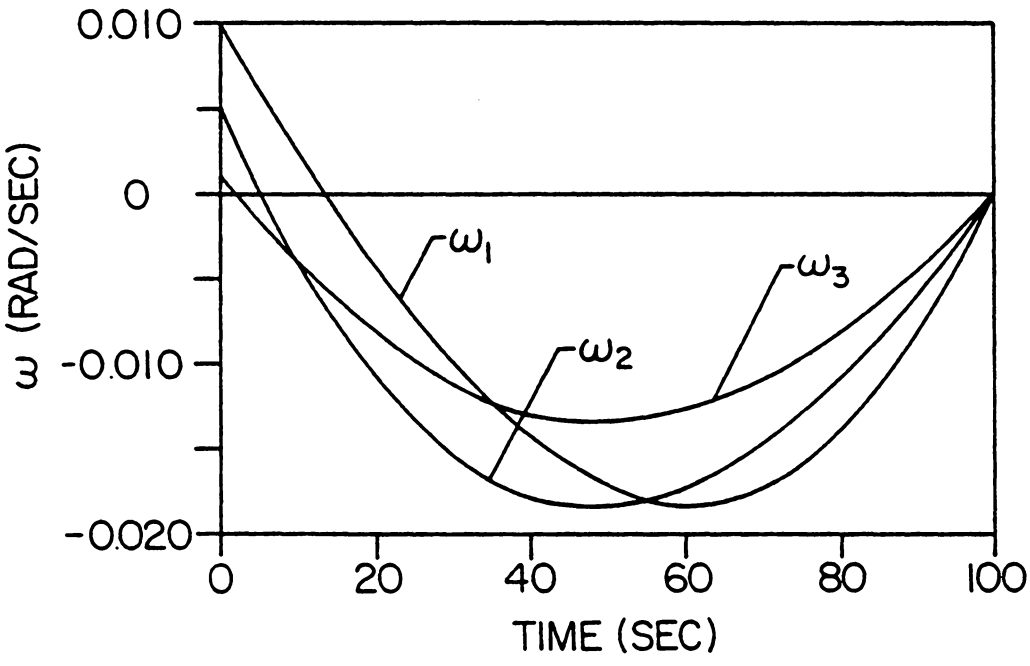

Fig. 5.1 (b) Spacecraft angular velocity components for Example 5.1.

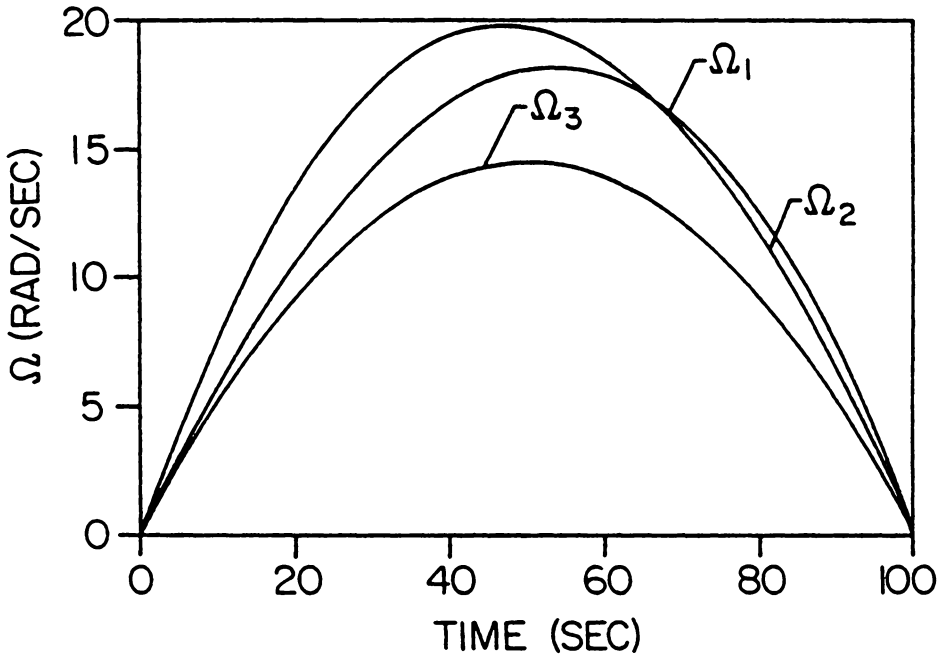

Fig. 5.1 (c) Wheel speeds for Example 5.1.

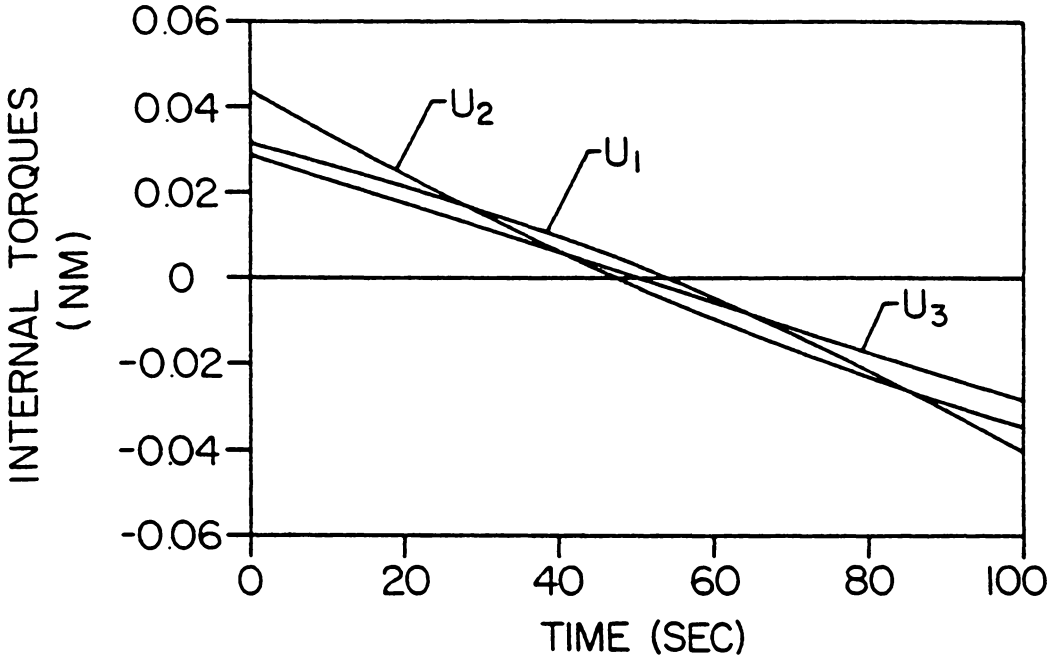

Fig. 5.1 (d) Optimal Internal Torques for Example 5.1.

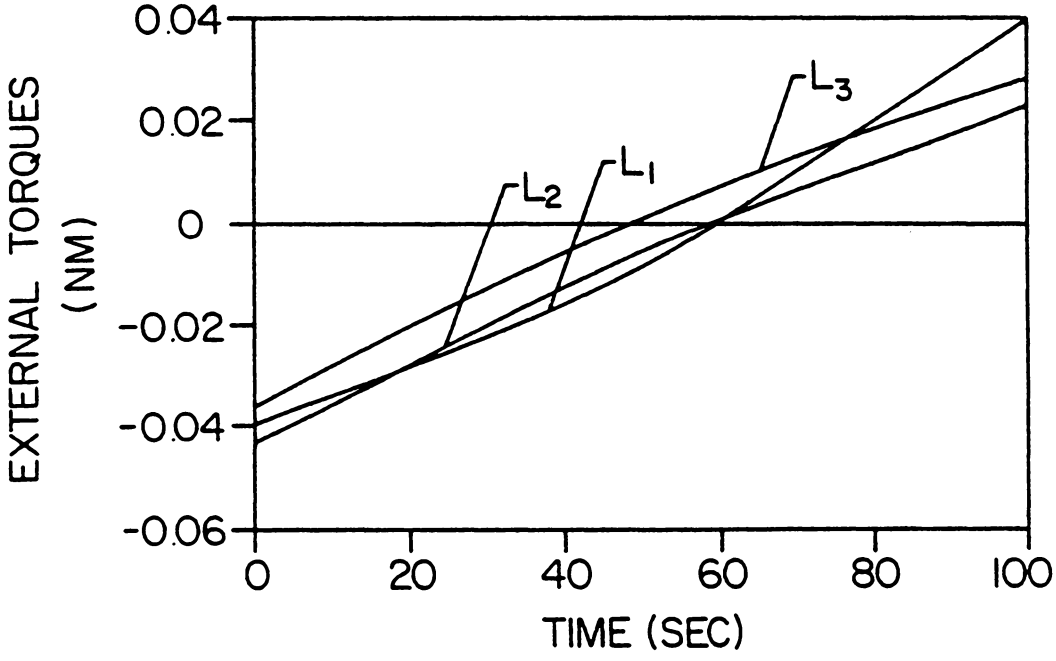

Fig. 5.1 (e) Optimal external torques for Example 5.1.

CHAPTER VI

CONCLUSIONS AND RECOMMENDATIONS

Some of the commonly used numerical schemes for the solution of nonlinear two-point boundary value problems have been discussed. Applications of these methods to a variety of optimal control problems are demonstrated via numerical examples of interesting optimal spacecraft large angle attitude maneuvers. Analytical studies of the problem of optimal large angle attitude maneuvers with external torques have yielded new insights which simplify the implementation of the numerical schemes. The optimal maneuver problem with reaction wheels has been formulated and solved for two different spacecraft configurations. The previous formulations have been mathematically extended to include external and internal torques simultaneously.

The various performance indices used for optimal control computations emphasize the following criteria:

a) minimum control effort

b) smoothness of the control and control rate

c) combination of (a) and minimum final state error

d) combination of minimum power required and smoothness of the control rate.

Of these criteria, the smoothness of the control rate is most important for the next generation large space structures which are fragile. Such controls excite the high frequency flexural modes of these spacecraft to a lesser degree in comparison to other control histories [37],[38].

During the course of this research we have identified the following problem areas which should be studied in the near future.

1) There is a need to understand the effects of performance index (weighting functions) and boundary conditions on stiffness of the resulting TPBVPs. Methods that avoid numerical integration and collocation would be extremely attractive also.
2) Obtaining globally optimal solutions, as opposed to locally optimal solutions to nonlinear optimal control problems is still a difficult task.
3) The dynamic models of spacecraft considered in this dissertation should be extended to include
   a) multiple reaction wheels (more than three), in skewed configurations to increase system realiability.
   b) flexible body dynamics to include the presence of booms, antennas, solar panels, and to include distributed control actuators.
4) The open loop optimal control solutions obtained here can be used to define good nominal maneuvers; feedback controls can then be determined in a perturbation sense, for onboard real time applications. However, there is interest in directly formulating nonlinear attitude maneuver controls in feedback form.

REFERENCES

1. Wertz, J. R. (ed.), Spacecraft Attitude Determination and Control, D. Reidel Publishing Co., Dordrecht, Holland, 1978.

2. Junkins, J. L., Rajaram, S., Baracat, W. A., and Carrington, C. K., "Precision Autonomous Satellite Attitude Control Using Momentum Transfer and Magnetic Torquing," The Journal of the Astronautical Sciences, Vol. xxx, No. 1, pp. 31-48, January-March, 1982.

3. Öz, H., and Meirovitch, L., "Optimal Modal-Space Control of Flexible Gyroscopic Systems," Journal of Guidance and Control, Vol. 3, No. 3, May-June 1980, Page 218.

4. Kaplan, M. H., Modern Spacecraft Dynamics and Control, John Wiley and Sons, New York, 1976.

5. Gebman, J. R., and Mingori, D. L., "Perturbation Solution of the Flat Spin Recovery of a Dual-Spin Spacecraft," AIAA Journal, Vol. 14, No. 7, July 1976, pp. 859-867.

6. Barba, P. M., and Auburn, J. N., "Satellite Attitude Acquisition by Momentum Transfer," American Astronautical Society, Paper No. AAS 75-043, Presented to the AAS/AIAA Astrodynamics Conference, Nassau, Bahamas, July 1975.

7. Junkins, J. L., "Some Recent Developments in Attitude Dynamics/Maneuver Strategies for Multiple Momentum Wheel Satellites," Proceedings of the Flight Mechanics/Estimation Theory Symposium, NASA, Goddard Space Flight Center, Greenbelt, MD, October, 1975.

8. Cochran, J. E., and Junkins, J. L., "Large Angle Satellite Attitude Maneuvers," Proceedings of the Flight Mechanics and Estimation Theory Symposium, NASA, Goddard Space Flight Center, Greenbelt, MD, April 1975.

9. Meyer, D., "On the Use of Euler's Theorem on Rotations for the Synthesis of Attitude Control Systems," NASA TN D-3643, September 1966.

10. Junkins, J. L., and Turner, J. D., "Optimal Continuous Torque Attitude Maneuvers," AIAA Paper No. 78-1400 presented at AIAA/AAS Astrodynamics Conference, Palo Alto, California, August 1978.

11. Skaar, S. B., and Kraige, L. G., "Single Axis Spacecraft Attitude Maneuvers Using an Optimal Reaction Wheel Power Criterion," accepted for publication in the Journal of Guidance, Control, and Dynamics, 1982.

12. Skaar, S. B., and Kraige, L. G., "Arbitrary Large-Angle Satellite Attitude Maneuvers Using an Optimal Reaction Wheel Power Criterion," AIAA Paper No. 82-1470, AIAA/AAS Astrodynamics Conference, San Diego, California, August 1982.

13. Skaar, S. B., "Arbitrary Large-Angle Satellite Attitude Maneuvers Using an Optimal Reaction Wheel Power Criterion," Ph.D. Dissertation, VPI & SU, August 1982.

14. Roberts, S. M., and Shipman, J. S., Two-Point Boundary Value Problems: Shooting Methods, American Elsevier Publishing Company, New York, New York, 1972.

15. Childs, B., "Codes for Boundary-Value Problems in Ordinary Differential Equations," Proceedings of a Working Conference May 14-17, 1978, in Lecture Notes in Computer Science, No. 76, Edited by G. Goos and J. Hartmanis.

16. Collatz, L., The Numerical Treatment of Differential Equations, 3rd ed. Springer-Verlag, Berlin, 1960.

17. Miele, A., "Recent Advances in Gradient Algorithms for Optimal Control Problems," Journal of Optimization Theory and Applications, Vol. 17, Dec. 1975.

18. Blank, D., and Shinar, J., "Efficient Combinations of Numerical Techniques Applied for Aircraft Turning Performance Optimization," AIAA Journal of Guidance and Control, Vol. 5, Mar. - Apr. 1982, pp. 124-130.

19. Miele, A., "Method of Particular Solutions for Linear, Two-Point Boundary-Value Problems," Journal of Optimization Theory and Applications, Vol. 2, No. 4, 1968.

20. Bryson, A. E., Jr., and Ho, Y. C., Applied Optimal Control, Halsted Press, Washington, D.C., 1975.

21. Miele, A and Iyer, R. R., "General Technique for Solving Nonlinear, Two-Point Boundary-Value Problems Via the Method of Particular Solutions," Journal of Optimization Theory and Applications, Vol. 5, No. 5, 1970.

22. Fox, L., Numerical Solution of Ordinary and Partial Differential Equations, Addison-Wesley, Reading, Mass., 1962.

23. Junkins, J. L., An Introduction to Optimal Estimation of Dynamical Systems, Sijthoff & Noordhoff, Leyden, The Netherlands, 1978.

24. Meirovitch, L., Computational Methods in Structural Dynamics, Sijthoff & Noordhoff, Leyden, The Netherlands, 1982.

25. Miele, A., Mangiavacchi, A. and Aggarwal, A. K., "Modified Quasilinearization Algorithm for Optimal Control Problem with Nondifferential Constraints," Journal of Optimization Theory and Applications, Vol. 14, No. 5, 1974, pp. 529-556.

26. Ojika, T., et al., "A Time - Decomposition Algorithm for a Stiff Linear Two-Point Boundary-Value Problem and Its Application to a Nonlinear Optimal Control Problem," Journal of Optimization Theory and Applications, Vol. 27, No. 2, Feb. 79.

27. Graney, L., "The Numerical Solution of Unstable Two-Point Boundary-Value Problems," Journal of Computational and Applied Mathematics, Vol. 3, No. 3, 1977.

28. Deuflhard, P., et al., "A Modified Continuation Method for Numerical Solution of Nonlinear Two-Point Boundary Value Problems by Shooting Techniques," Numerical Math., 26, 327-343 (1976).

29. Orava, P. J., and Lautala, A. J., "Back-and-Forth Shooting Method for Solving Two-Point Boundary-Value Problems," Journal of Optimization Theory and Applications, Vol. 18, No. 4, April 1976.

30. Miele, A., et al., "Solution of Two-Point Boundary-Value Problems with Jacobian Matrix Characterized by Large Positive Eigenvalues," Journal of Computational Physics, 15, 117-113 (1974).

31. Morton, H. S., Junkins, J. L., and Blanton, J. N., "Analytical Solutions for Euler Parameters," Celestial Mechanics, Vol. 10, (1974), pp. 287-301.

32. Whittaker, E. T., A Treatise on the Analytical Dynamics of Particles and Rigid Bodies," Dover, New York, 1944, pp. 10-11.

33. Morton, H. S., Unpublished private communication with J. L. Junkins, December 1974.

34. Margulies, G. and Aubrun, J. N., "Geometric Theory of Single-Gimbal Control Moment Gyro Systems," The Journal of the Astronautical Sciences, Vol. 26, No. 2, pp. 159-191, April-June 1978.

35. Vadali, S. R., and Junkins, J. L., "Spacecraft Large Angle Rotational Maneuvers with Optimal Momentum Transfer," AIAA Paper No. 82-1469, presented at AIAA/AAS Astrodynamics Conference, San Diego, California, August 1982.

36. Kraige, L. G., and Junkins, J. L., "Perturbation Formulations for Satellite Attitude Dynamics," Celestial Mechanics, Vol. 13 (1976), pp. 39-64.

37. Junkins, J. L., "Optimal Feedback Slewing of Flexible Spacecraft," Technical Comment, AIAA Journal of Guidance, Control, and Dynamics, Volume 5, No. 3, May-June 1982.

38. Turner, J. D., and Chun, H. M., "Optimal Distributed Control of a Flexible Spacecraft Using Control-Rate Penalties in the Controller Design," AIAA Paper No. 82-1438, presented at AIAA/AAS Astrodynamics Conference, San Diego, California, August 1982.

39. Kirk, D. E., Optimal Control Theory. An Introduction, Prentice Hall, New Jersey, 1970.

APPENDIX A

PONTRYAGIN'S NECESSARY CONDITIONS

Summary of necessary conditions for optimality for a system: $\dot{x} = f(x,u,t)$, (A1)

where x is an n-vector of states

u is an m-vector of controls ($m \leq n$)

f is an n-vector of nonlinear functions

and a performance index:

$$J = \phi[x(T),T] + \int_0^T L[x(t),u(t),t]dt. \tag{A2}$$

are presented below. The Hamiltonian (**H**) is defined as

$$\mathbf{H} = L(x(t),u(t),t) + \lambda^T(t)f[x(t),u(t),t], \tag{A3}$$

where $\lambda(t)$ is an n-vector of Lagrange multipliers or co-states.

The necessary conditions for optimality of u are

i) $$\dot{x} = \left\{\frac{\partial \mathbf{H}}{\partial \lambda}\right\}^T = f(x,u,t), \tag{A4}$$

ii) $$\dot{\lambda} = -\left\{\frac{\partial \mathbf{H}}{\partial x}\right\}^T = -\left\{\frac{\partial f}{\partial x}\right\}^T\lambda - \left\{\frac{\partial L}{\partial x}\right\}^T, \tag{A5}$$

iii) u(t) is chosen to extremize the Hamiltonian

(Control constraints are not included):

$$\left\{\frac{\partial \mathbf{H}}{\partial u}\right\}^T = \left[\frac{\partial f}{\partial u}\right]^T\lambda + \left\{\frac{\partial L}{\partial u}\right\}^T = 0. \tag{A6}$$

Eqs. (A4), (A5) and (A6) constitute 2n differential equations and m algebraic equations for (2n + m) states, co-states and controls.

Boundary conditions:

The states are initially specified, then

$x(0) = x_0$ (n boundary conditions).

Either the states are specified at the final time, then

$x(T) = x_T$ (n boundary conditions),

or they are free, leading to

$$\lambda^T(T) = \{\frac{\partial \phi}{\partial x}\}|_{t=T} \text{ (n boundary conditions).}$$

More general formulations and necessary conditions are presented by Kirk [39].

The vita has been removed from the scanned document

SOLUTION OF THE TWO-POINT BOUNDARY VALUE PROBLEMS OF OPTIMAL SPACECRAFT ROTATIONAL MANEUVERS

by

Srinivas R. Vadali

(ABSTRACT)

Numerical schemes for the solution of two-point boundary value problems arising from the application of optimal control theory to mathematical models of dynamic systems, are discussed. Optimal control problems are formulated for rotational maneuvers of multiple rigid body, asymmetric spacecraft configurations with both external torques and/or internal torques. Necessary conditions for optimality are derived through Pontryagin's principle; solutions to the problems are obtained numerically. Comparison studies using competing numerical methods and various choices of performance indices are reported.